A Cenozoic shift from extensional to strike-slip tectonics in the central Mediterranean Sea

Giacomo Mangano[a,c], Tiago M. Alves[b], Dario Civile[c], Salvatore Critelli[a], Massimo Zecchin[c]

a Department of Environmental Engineering, University of Calabria, 87036, Arcavacata di Rende, CS, Italy

b 3D Seismic Laboratory – School of Earth and Environmental Sciences, Cardiff University, CF10 3AT, United Kingdom

c National Institute of Oceanography and Applied Geophysics – OGS 34010 Sgonico, TS, Italy

Abstract

High-resolution 3D seismic reflection data, structural interpretations and expansion index analyses are combined in this work to explain the mechanisms that drove a newly discovered shift from extensional to strike-slip tectonics in the central Mediterranean region. In the Crotone Basin, Early Pliocene extension predominated at first as proven by the nucleation of N- to NE-striking normal faults bounding half-graben basins and tilt blocks. Fault length reached ~13 km, with associated half-grabens being 5 to 8 km wide and up to 2.5 s TWT deep. Extensional tectonics at this stage followed tectonic collision between the Calabrian margin and the Apulian foreland; the removal of dense lithospheric mantle induced sharp elevation gradients and a rapid uplift of continental crust in the study area, promoting isostatic imbalances that ultimately led to extensional orogenic collapse. This same phase of extension was accompanied by the reactivation of inherited fault systems, which occurred together with the forward migration of the Calabrian Arc and oceanization of the Tyrrhenian Sea. Conversely, normal-oblique to strike-slip faulting has predominated offshore Crotone since the Late Pliocene as recorded by the development of elongated (up to ~ 22 km long) and narrow (~ 3 km wide) NW-trending pull-apart basins. Structural styles have since then been influenced by rheological contrasts between the continental Apulian foreland and Ionian oceanic lithosphere, which activated a broad WNW-striking shear corridor. As a corollary of this work, modern structural and kinematic evidence indicates that fault segments within this shear corridor are arranged in an *en echelon* geometry and act as conjugate structures accommodating the progressive fragmentation of the overriding Apulian plate. On a broader scale of analysis, the transition from pure extension to strike-slip tectonics documented offshore Crotone is associated with the differential subduction of heterogeneous foreland domains, a phenomenon that reflects the dynamic evolution of the central Mediterranean backarc system as a whole.

Keywords: Central Mediterranean Sea, Calabria, Strike-slip, Extension, Tectonics, Crotone Basin.

1. Introduction

Normal faults are the hallmark structures of continental rifting, evolving as the lithosphere is progressively thinned due to the interplay between tectonic forces and inherited lithospheric heterogeneity (Jackson and McKenzie, 1983; Ebinger et al., 1993; Gawthorpe and Leeder, 2000; Brune et al., 2023; Civile et al., 2024). As rifting localizes, brittle deformation is preferentially accommodated via the nucleation and growth of normal faults, a process that marks a fundamental change from a stable plate interior to nascent plate boundaries (Jackson and McKenzie, 1983; Peacock and Sanderson, 1991; Elliott et al., 2017; Strugale and Cartwright, 2022; Brune et al., 2023). Importantly, normal faults can also develop during orogenic fragmentation, i.e. in the context of compressional tectonics and orogenesis (Dewey, 1988; Rossetti et al., 2005; Cavalcante et al., 2024; Pollock, 2025), whereby a combination of gravitational body forces acting on overthickened crust, thermal weakening and crustal delamination, are able to drive extensional deformation over previously accreted lithosphere (Bird, 1978; Sawyer, 1985; Dewey, 1988; England and Houseman, 1988; Rossetti et al., 2005; Heron et al., 2016; Cavalcante et al., 2024; Pollock, 2025).

Extensional detachments in post-orogenic settings are often localized along inherited weakness zones, which are reactivated when lithospheric thickening changes to gravitational spreading and tectonic extension (Dalmayrac and Molnar, 1981; Selverstone, 1988; Dewey, 1988; Labrousse et al., 2011; Teyssier et al., 2005; Rossetti et al., 2005; Cavalcante et al., 2024; Pollock, 2025). In some cases, normal oblique and strike-slip movements reflect the presence of lithospheric discontinuities and contrasting rheological properties between foreland domains, with both being able to cause important strain partitioning along horizontal and vertical shear components (Finetti and Del Ben 1986; Lanzafame and Bousquet 1997; Gvirtzman and Nur 1999; Argnani 2000; Doglioni et al. 2001; Rosenbaum and Lister 2004; Finetti 2005). This means that important lithospheric deformation associated with subsidence, horizontal stretching, and localized crustal thinning may arise from the lateral displacement between tectonic plates, where strike-slip fault systems are formed (Molnar and Tapponnier, 1975; Peacock and Sanderson, 1995; Tapponnier et al., 2001; Dooley and Schreurs, 2012).

The Crotone Basin is a forearc basin of the central Mediterranean (southern Italy) that is also a constituting part of the Calabrian Accretionary Wedge; yet, it has been dominated by extensional and transtensional tectonics since the Pliocene (Van Dijk et al., 2000; Massari and Prosser, 2013, Zecchin et al., 2020; Civile et al., 2022; Mangano et al., 2022; 2023a; 2024) **(Figure 1a,b).** The presence, in the Crotone Basin, of normal faults with orientations that differ markedly from Quaternary NW and NNW faults, is still poorly understood. Some of these Quaternary faults can be attributed to upper-crustal gravitational collapse (Zecchin et al., 2018; Mangano et al., 2020; 2021; 2023b; Ceramicola et al. 2024), but the majority are located far from well-known gravitational complexes, revealing kinematics indicators that are not associated to slope instability.

The aim of this study is to discriminate between Early Pliocene and younger faults in the Crotone Basin, addressing the tectonic drivers and boundary conditions that controlled their evolution. The focus is placed on the offshore sector of the Rossano–San Nicola fault zone, a NW-trending regional-scale strike-slip structure that defines the northern boundary of the Crotone Basin and evolved in connection with the southeastward migration of the Calabrian Accrectionary Wedge (**Figure 1b).** Three-dimensional (3D) seismic data and a suite of exploration wells are therefore used in this work to address three fundamental research questions:

a) What are the kinematic differences between Early Pliocene and Late Pliocene-Quaternary fault systems?
b) How do fault geometries, orientations, and associated syn-tectonic strata relate to differing tectonic regimes?
c) What role did orogenic processes and lithospheric heterogeneity play in localizing deformation during the tectonic evolution of the Calabrian Arc?

Answers to these questions are contextualized within the broader geodynamic framework of the central Mediterranean, and add crucial information regarding the complex evolution of this region **(Figure 1)**.

2. Geological setting

2.1 *Tectonic Framework of the Calabrian Accretionary Wedge*

The central Mediterranean region is one of the most complex and dynamic subduction systems of the Alpine-Mediterranean belt, having been shaped throughout the Cenozoic by slab retreat, back-arc extension, and plate convergence (Dewey et al. 1989; Guerrera et al. 1993, 2012; Schettino and Turco 2011; Guerrera and Martín-Martín 2014; Hosseinpour et al. 2016; Royden and Faccenna, 2018; van Hinsbergen et al. 2020; Critelli and Criniti 2021; Critelli et al., 2021; Critelli and Martín-Martín 2022, 2024; Belayouni et al. 2023). Against this backdrop, the subduction zone that marks the modern boundary between the Eurasia and Africa plates runs parallel to the North African coast from Cyprus to Southern Greece, turning northward at the eastern part of the central Mediterranean, in the Ionian Sea (Faccenna et al., 2001; 2004; Minelli and Faccenna, 2010; Polonia et al., 2011). The geodynamic history of the central Mediterranean is *per se* closely related, for the past 50 Ma, to episodes of retreat and rollback of its NW-dipping oceanic lithosphere, and has led to orogenic accretion along the Kabylia (Algeria), Calabrian and Apennine (Italy) mountain ranges. Importantly, the opening of the back-arc Liguro-Provencal and Tyrrhenian basins occurred further west at the same time tectonic convergence ensued (Malinverno and Ryan, 1986; Royden, 1993; Chaumillon and Mascle, 1997; Wortel and Spakman, 2000; Faccenna et al., 2001; 2004; Minelli and Faccenna, 2010; Polonia et al., 2011).

The Calabrian Accretionary Wedge (CAW), located in the northern part of the Ionian Sea near Italy, is a SE-verging tectonic domain of a subduction system that resulted from the scraping of the descending Ionian oceanic lithosphere under continental crust of the Calabrian Arc – the latter comprising an arcuate nappe-stack of ophiolites, pre-Alpine basement units, remnants of Mesozoic-Cenozoic sediments, and metamorphozed rocks (Bonardi et al., 2001; Critelli et al., 2018) (**Figure 1a**). The CAW accreted an area roughly 300 km wide to 400 km long that is located between the Maghrebides thrust belt and the Malta Escarpment to the SW, and the Apulian foreland and Apulia Escarpment to the N and the

NE (Rossi and Sartori, 1981; Barone et al., 1982; Finetti, 1982; Sioni, 1996; Faccenna et al., 2001; 2004; Minelli and Faccenna, 2010) (**Figure 1a).** The CAW is itself limited to the SE by the Mediterranean Ridge, an evolving accretionary complex resulting from ongoing convergence between Africa and Eurasia, and from the concomitant southward motion of the Aegean microplate (Bonardi et al., 2001; Polonia et al., 2002; Camerlenghi et al. 2020; Mouslopoulou et al. 2025; Chizzini et al., 2025) (**Figure 1a**).

Authors such as Minelli and Faccenna (2010), Polonia et al. (2011), Gallais et al. (2012) and Maesano et al. (2017) have sub-divided the CAW into four tectonic domains which, from the SE to the NW, comprise: i) the Ionian foreland basin, an area made up of Mesozoic to Plio-Quaternary sediments located between the Mediterranean Ridge and the Malta Escarpment, inferred to be a relic of the Ionian Abyssal Plain, ii) the outer accretionary wedge, composed of Messinian to Plio-Quaternary sediments representing the frontal part of the wedge, iii) the inner accretionary wedge formed by pre-Messinian to Plio-Quaternary successions and constituting the inner portion of the wedge, and iv) the Crotone-Spartivento Basin, filled by Serravallian to Quaternary deposits accumulated in a forearc position relative to the CAW (**Figure 1a,c)**. In addition to this four-fold subdivision, the CAW is partitioned into eastern and western lobes, which present differences in tectonic architecture and structural complexity. These two lobes are separated by the Ionian Fault System, a major structural lineament that acts as a first-order boundary within the CAW (**Figure 1a**).

2.2 *Miocene evolution of the Crotone Basin*

The Crotone Basin is separated from the Spartivento Basin by the Punta Stilo Swell (Mangano et al., 2022) and overlies both inner accretionary-wedge sediments and crystalline basement rocks (Rossi and Sartori, 1981; Minelli and Faccenna, 2010) (**Figure 1a,b)**. Its origin dates to the Middle Miocene (Serravallian), when continental rifting migrated from the western margin of the Sardinia-Corsica block to the southeast after the end of the Liguro-Provencal oceanic spreading phase (Kastens et al., 1988; Sartori, 1990). Its development was controlled by the NW-striking Rossano–San Nicola and Petilia–Sosti fault zones, which imposed distinct phases of deformation and subsidence inside the basin (Meulenkamp et al., 1986; Van Dijk, 1991, 1994; Van Dijk and Okkes, 1991; Muto et al., 2014; Van Dijk et al., 2000; Civile et al., 2022) **(Figure 1b**). Such structures are, in turn, confined within a broader shear system, the Sibari and Catanzaro strike-slip zones, structures that were initiated in the Early Pliocene and accommodated the clockwise rotation of the Calabrian Arc during its southeastward migration (Del Ben et al., 2008) (**Figure 1a**).

2.3 *Messinian Salinity Crisis and related tectonic inputs*

The Crotone Basin was significantly affected by the Messinian Salinity Crisis (MSC), which followed an initial phase of tectonic extension and frontal accretion of the CAW. In the geodynamic framework considered in this work, the MSC was triggered by the progressive tectonic confinement and closure of the Atlantic–Mediterranean gateways (Betic and Rif corridors), which severely reduced water exchange with the Atlantic Ocean and led to extreme basinwide evaporative drawdown (Roveri et al., 2014; Flecker et al., 2015; Krijgsman et al., 2018; Krijgsman et al., 2024). The sea-level drop associated with this crisis was enough to promote the flexural rebound of the lithosphere near the CAW, thus generating strike-slip faults that accommodated up to 1600 m of evaporites and produced a prominent, basinwide Intra-Messinian Unconformity (IMU) dated at 5.6–5.55 Ma (DeCelles and Cavazza, 1995; Cavazza and DeCelles, 1998; Krijgsman et al., 1999; Hilgen et al., 2007; Govers et al., 2009; Zecchin et al., 2020; Borrelli et al., 2021, 2022; Mangano et al., 2024). Evaporite deposition facilitated, at the same time, the southeastward advance of the CAW by over 100 km along a salt-rich basal décollement (Minelli and Faccenna, 2010). The evaporitic substratum also promoted the deformation of the basinal successions located at the front of the Messinian evaporites, which subsequently became incorporated into the post-Messinian outer accretionary wedge (Polonia et al., 2011, 2016; Gallais et al., 2012; Camerlenghi et al., 2020; Chizzini et al., 2025). This phase of accretionary wedge advance was then followed by a contractional/transpressional episode that was probably triggered by a reduction in the wedge's taper below its critical value, as marked by a landward migration of deformation and resulting out-of-sequence internal shortening in the CAW (Minelli and Faccenna, 2010; Polonia et al., 2011). In the Crotone Basin, this tectonic phase is expressed by the development of the Upper Messinian Unconformity (UMU) at 5.42 Ma. Importantly, it also marks the transient coupling between the northeastern Calabrian Arc and the Apulian margin at the very end of the Miocene (Massari and Prosser, 2013; Zecchin et al., 2013, 2020) (**Figure 2**).

2.4 *Pliocene-Quaternary evolution*

Backarc extension related to Ionian plate subduction started in the study area after the late Messinian contractional/transpressional events as the Vavilov sub-basin opened in the Tyrrhenian back-arc **(Figure 1a)**. Seafloor spreading occurred at first in the Vavilov sub-basin at around 4.3 Ma, recording a fast extensional rate of 8 cm/yr (Guillaume et al., 2010). At the same time, the CAW witnessed fast frontal growth above the weaker Messinian salt, thus reducing the accretionary wedge's taper angle, lowering the topographic slope, and increasing its total length by more than 200 km (Minelli and Facenna, 2010). This event triggered important subsidence in the Crotone Basin, as testified by the accumulation of up to 1000 m of Zanclean mudstones (Zecchin et al., 2012; 2015; 2020) **(Figure 3).**

After another (Pliocene) phase of contractional/transpressional tectonics, which resulted in the development of the basinwide Mid-Pliocene Unconformity (MPCU; Basso et al., 2021; Zecchin et al., 2015, 2020) (**Figure 2**) and the concomitant onset of large mass-transport complexes (Zecchin et al., 2018; Mangano et al., 2020; 2021; 2022; 2023a; b; 2024), the Crotone Basin experienced a phase of tectonic stretching in the Piacenzian (latest Pliocene). This phase was contemporaneous with the final episode of ocean spreading in the Vavilov sub-basin, which probably ended at ~2.6 Ma (Feraud, 1990). It led to the accumulation of the lower part of the Cutro Clay in the distal parts of the Crotone Basin (Zecchin et al., 2006; 2012) (**Figure 2**). This latest Pliocene pulse of subsidence was again interrupted by a local contractional episode at the start of the Quaternary, in the early Gelasian (ca. 2.4 Ma), as marked by an Early Pleistocene unconformity (EPSU). Contractional tectonics was likely associated with the end of the movement of northern Calabria towards the Apulian plate. It also marked the end of the Vavilov sub-basin's development (Zecchin et al., 2012; Basso et al., 2021).

Rapid tectonic subsidence continued during the middle Gelasian in parallel with the ultra-fast opening of the Marsili sub-basin, with spreading rates reaching up to 19 cm yr^{-1} at this time (Nicolosi et al., 2006; Guillaume et al., 2010). As a result, a ~20° clockwise rotation and southeastward migration of the Calabrian Arc occurred at this time due to trench rollback and back-arc extension (Sagnotti, 1992; Scheepers et al., 1994; Speranza et al., 2000, 2011; Mattei et al., 2004, 2007; Nicolosi et al., 2006; Mattei et al., 2004, 2007; Chiarabba et al., 2008; Zecchin et al., 2012). Subsequently, transpressional NW-striking shear zones were formed to accommodate the differential motion between the northern and southern sectors of the Calabrian Arc. Marked stratigraphically by a Mid-Pleistocene Unconformity (MPSU) dated at ~1.1 Ma, such an accommodation was made easier by the presence of lithospheric-scale tear faults at the boundary between the Apulian and Ionian forelands (Del Ben et al., 2008; Zecchin et al., 2012, 2015).

A final episode of transtensional tectonics linked to a renewed, low rate spreading of the Marsili sub-basin occurred after 1.1 Ma. Rapid tectonic uplift affected the Crotone Basin soon after at ~0.45 Ma, with diverse mechanisms being proposed for its onset. These include slab break-off and isostatic rebound (Spakman, 1986; Wortel and Spakman, 2000), whereas convective removal of the lithospheric root has been proposed by Doglioni (1991) and Gvirtzman and Nur (2001) amongst other authors.

3. Data and methods

3.1 *Seismic and borehole data*

The main dataset in this work is part of a post-stack time-migrated (PSTM) 3D seismic volume provided by ENI Natural Resources. It covers part of the offshore sector of the Crotone Basin, spanning an area of c. 535 km^2 of the continental shelf and slope off Calabria (**Figures 1 and 3).** The seismic cube consists of 4,652 inline and 2,908 crossline traces with a regular inline and crossline spacing of 15 m.

The imaging window of the seismic data is 5.0 s two-way time (TWT), while each seismic trace has 1251 samples and was sampled at an interval of 4 ms. Based on the borehole data used in this study, average interval velocities were estimated at approximately 1,800 m/s for Unit A, 2,300 m/s for Unit B, and 3,300 m/s for Unit U (see section 4.1). By also estimating a dominant frequency of ~48 Hz, within a bandwidth range of approximately 2.75 Hz to 80 Hz, vertical resolution was calculated to vary from ~ 9.4 m in Unit A to ~17.2 m in the deeper Unit U.

Two key seismic horizons, H1 and H2, together with the seafloor, were mapped and correlated to the regional stratigraphic framework based on data from nine (9) exploration wells and the tectono-stratigraphic scheme of Critelli (1999), Zecchin et al. (2020) and Mangano et al., (2023a) **(Figures 2, 3 and 4).** These horizons were selected because they show characteristic high-amplitude signatures that can be traced consistently across the entire study area, enabling a clear separation between the Early Pliocene and Late Pliocene–Recent intervals. They effectively bracket the temporal window of importance to this study. Essential lithological descriptions and depth measurements from the rotary table (RT) were extracted from these wells, allowing for an accurate time-depth conversion and calibration of the seismic horizons. These borehole data enabled a robust correlation of H1 and H2 with the regional stratigraphic framework.

3.2 *Seismic Interpretation*

Seismic interpretation was completed in the time domain using Schlumbergers' Petrel®. The analysis was guided by the seismic-stratigraphic principles in Mitchum et al. (1977), which emphasize the recognition of reflection patterns corresponding to lithological variations and unconformities. Key unconformities bound seismic units that are distinguished by variations in seismic facies, configuration patterns, reflector terminations, depth, and thickness.

The interpreted borehole data were imported into Schlumberger's Petrel® with their check-shots, allowing the visualization of their measured depth - defined as the depth from the rotary table (RT) - within the time domain. This integration enabled an accurate time-to-depth calibration of the seismic data, and precise correlations between seismic reflectors and well data. For units not fully penetrated by exploration wells, their ages and lithologies were derived from published work on the Crotone Basin's stratigraphy (Critelli, 1999; Zecchin et al., 2020; Mangano et al., 2023a) (**Figure 2**).

Faults were interpreted according to breaks in continuity (and associated offsets) of seismic reflectors. Although seismic amplitude displays are routinely used to trace out faults in profiles, other seismic attributes such as variance were applied, especially in plan view. Variance measures the degree of contrast between seismic traces and transforms a volume characterized by seismic continuity into one that emphasizes discontinuities, effectively delineating structural and stratigraphic boundaries (Brown, 2004). Knowing that faults reveal themselves in seismic data as trace-to-trace variations, they are identified in areas characterized by high variance coefficients. A total of 12 major faults were interpreted across the study area, with their orientation graphically displayed in a rose diagram.

The interpretations of horizons and faults were further used to generate structural surfaces and thickness maps, providing insights into basin architecture and deformation history.

3.3 *Fault growth analyses using the Expansion Index (EI) method*

Fault activity was assessed via measuring their Expansion Indices, a quantitative approach that assesses the growth history and nucleation of normal faults (Thorsen, 1963, McCulloh, 1988; Edwards, 1995). Expansion Index (EI) is defined as the ratio of the stratigraphic thickness of a seismically resolved unit on a fault's hanging-wall depocenter relative to its thickness on immediate footwall blocks (Thorsen, 1963; Pochat et al., 2009). The method provides a robust way to assess fault activity through the systematic measurement of syn-tectonic strata thickness accumulated near mapped faults. Hence, an EI value of 1 indicates no variations in stratigraphic thickness across a fault, suggesting that it was inactive during the deposition of a given unit. Conversely, EI values greater than 1 document stratigraphic thickening on the immediate hanging-wall of a fault, i.e. they relate to fault movement during deposition (Thorsen, 1963; Cartwright et al., 1998; Rouby et al., 2003; Hongxing and Anderson, 2007). The measurement of EI across all 12 mapped faults allowed for a detailed reconstruction of fault growth patterns and their role in controlling sediment accumulation.

Data were sampled every line at the maximum resolution of 15 m as suggested by Tao and Alves (2019).

4. Results

This section gives an account of the seismic stratigraphic units offshore the Crotone Basin based on the comprehensive seismic and borehole data interpreted in this work **(Figure 3).**

4.1 *Seismic-stratigraphy*

Horizon H1 is a high-amplitude, wavy reflector with poor lateral continuity (**Figures 5 and 6**). It is dissected by an extensional system formed by NW-oriented normal faults, which dip approximately 55–70° and define two narrow and elongated depocenters. This same extensional system defines two structural highs in the central and southwestern parts of the study area, both with a minimum TWT depth of 417 ms (**Figure 4a**). A broader depocenter occurs to the north, where it reaches a maximum TWT depth of 2651 ms (**Figure 4a)**. On most of the interpreted seismic profiles, horizon H1 is sub-parallel to the strata immediately above and below (**Figures 5 and 6)**.

Horizon H2 is a high-amplitude, discontinuous and deformed seismic reflector that defines structural lows and highs across the downthrown and upthrown sides of normal faults, i.e. F1 to F4 and F11 and F12 (**Figures 4b, 5 and 6).** Its TWT depth varies from 962 ms to 2983 ms (**Figure 4b**). Through most of the study area, H2 truncates its underlying strata and is onlapped by seismic reflections at its top (**Figures 5 and 6**).

Horizons H1 and H2 are both basinwide seismic-stratigraphic markers that correlate with the MPCU and UMU, respectively **(Figure 2).** They divide the imaged successions into Units A, B and U (**Figures 5 and 6)**.

Unit A

Unit A consists of parallel to sub-parallel internal reflections with a variable amplitude and continuity, changing laterally into inclined and wavy reflections (**Figures 5 and 6)**. Unit A tops half-grabens filled by Unit B (**Figures 5b and 6c)** and is thicker on the immediate hanging-walls of faults F7 to F10 (**Figure 6a, b)**. In contrast, it has a fan-like geometry near faults F5 and F6 (**Figures 5a)**. The unit is bounded at its top by the seafloor and at its base by Horizon H1 (**Figures 5 and 6)**.

The thickness of Unit A varies across the study area, with values ranging from a maximum of approximately 1530 ms in fault-controlled depocenters to a minimum of 144 ms over structural highs (**Figure 7a**). The thickest accumulations are found in the northern and northwestern sectors of the study area, stressing how important was tectonic subsidence near fault F3 (**Figure 7a**). In turn, important thinning occurs in Unit A between the two later depocenters, a character highlighting the presence of NW-striking footwall blocks between depocentres. Unit A also becomes thinner towards the south (**Figure 7a**).

Based on the available borehole stratigraphic data, Unit A correlates with shelf to slope claystones and siltstones in the Cutro Clay, which have accumulated in the study area since the latest Pliocene (Piacenzian; Zecchin et al., 2020) (**Figures 2 and 3**).

Unit B

Unit B is composed of parallel to sub-parallel internal reflections with moderate continuity and low to high amplitude. They change locally into chaotic facies (**Figures 5b and 6a)**. In some areas, seismic reflections present onlap and downlap terminations against Horizon H1, hinting at local sediment progradation (**Figures 5a, b, c and 6b)**. Unit B is bounded at its top by Horizon H1 and at its base by Horizon H2 (**Figures 5 and 6)**. It reveals growth strata on the immediate hanging-wall of normal faults (**Figure 5a, b, d**), although still presenting other important changes in thickness. In fact, Unit B records maxima in thickness near the central, southern, and northwestern sectors of the study area where it reaches values of 1425 m in well-defined depocenters (**Figure 7b**). These depocenters coincide with hanging-wall blocks formed near major N-, NNE-, and NE-striking normal faults, i.e. F1, F2, F3, F4, F11, and F12 (**Figure 7b**). Unit B is much thinner over structural highs, particularly across the uplifted footwall blocks of the latter faults, where it is absent (**Figure 7b**). The number of normal faults cross-cutting Unit B is also greater than in Unit A, with minor normal faults being observed throughout the study area within the former unit (**Figures 5 and 6).** Fault displacement within this interval is minor, however, not disrupting the continuity of seismic reflections within Unit B.

Based on the available borehole data, Unit B correlates with the Lower Pliocene shelf to slope mudstones of the Cavalieri Marl (Zecchin et al., 2020) (**Figures 2 and 3**).

Unit U

The lowermost Unit U is characterized by a diverse range of seismic reflection patterns, including transparent to high-amplitude internal reflections with variable continuity (**Figures 5 and 6**). The unit is predominantly chaotic, with internal reflections locally dipping towards the SW, SE, and NE (**Figures 5 and 6**). Its TWT thickness reaches a maximum value of *c.* 4.0 s, but varying significantly across the study area (**Figure 5c**). In addition, Unit U is crosscut by both low- and high-angle faults, with those extending into the deeper section being associated with the Rossano-San Nicola Fault Zone, as reported by Mangano et al. (2023b) and Mangano et al. (2024) **(Figures 5a and 6c).** Its upper boundary is horizon H2 (**Figures 5 and 6)**.

Unit U correlates with deposits ranging in age from the Mesozoic to the Messinian based on the regional stratigraphic framework presented by Critelli (1999), Zecchin et al. (2020) and Mangano et al. (2023a), and include a thick carbonate succession with intercalated organic-rich shales. The upper part of the unit corresponds to mass-wasting deposits and shelf-to-slope mudstones, with the latter reflecting sedimentary processes associated with progressive basin subsidence and deepwater deposition (Zecchin et al., 2020) (**Figure 2**).

4.2 Fault geometry and distribution

Seismic interpretation reveals a network composed of 12 main faults (F1–F12), each with particular kinematic expressions and structural styles. Their orientations are summarized in the accompanying rose diagrams in **Figure 8a**. They all fall within the offshore prolongation of the Rossano-San Nicola Fault Zone (**Figures 8)**. Two-way time structural maps show that faults F1 to F4, and also F11 and F12, strike predominantly to the NE, N, and NNW, bounding a series of depocenters filled by the Lower Pliocene Unit B (**Figure 4a)**. In contrast, faults F5 to F10 strike NW–SE and show variable lengths, bounding narrow, elongated depocenters that are only filled by Unit A (Late Pliocene-Quaternary) (**Figure 4b**). Faults F1, F5 and F6 are sigmoidal on variance time slices, a geometry typically found where the shear strain is partitioned in a direction parallel to the strike of the fault planes (**Figure 9**). These faults are also are filled by strata with a divergent, concave-upward geometry (**Figure 5a**). When imaged together, faults F1, F5, and F6 reveal an *en echelon* geometry in map view, with well-developed splay systems or horsetail geometries at their tips (**Figure 9**). These splays are parallel to slightly oblique to the strike of master faults, suggesting localized strain partitioning near fault tips and their damage zones (**Figure 9**)**.** The presence of releasing fault stepovers is also recognized near F7 and F8 (**Figure 6a**). Similarly, faults F7 to F10 accommodate localized transtension and led to the formation of local pull-apart sub-basins within a larger NW-striking fault zone (**Figure 6)**.

Faults F2, F4, F11, and F12 are relatively straight and form nearly parallel arrays (**Figures 5b, 5c and 6c**). These faults bound tilt blocks and their adjacent half-graben basins, and are associated with drag folding in their hanging-wall domains as observed in **Figures 5b and 6c**. Selected variance time slices further confirm that faults F2 and F4 are linear and form parallel fault arrays **(Figure 10a,c**).

Seismic profiles also reveal that the upper tips of faults F2 and F12 terminate within Unit B (**Figures 5a and 6c),** while F1 and F11 extend slightly above the horizon MPCU (**Figures 5a and 6c**). In contrast, faults F3 and F4, as well as the F5–F10 fault system, propagate through Unit A in its entirety (**Figures 5a, c, d and 6a, b)**.

4.3 *Expansion indexes*

Expansion indices (EI) for the mapped faults F1 to F12 are characterized by their marked variability (**Figure 11**). The highest EI value (5.65) was measured for fault F2, while the lowest values (0.67) were calculated for faults F9 and F10. Variations in EI across different units were also recorded for the analyzed faults. For instance, faults F1, F2, F11, and F12 reveal an increase in EI with depth, significantly exceeding 1.0 in Unit B (**Figure 11**). In contrast, faults F3 and F5 to F10 show an increase in EI towards the seafloor. Among the latter, only fault F3 shows a consistent increment in the thickness of hanging-wall strata compared to its footwall. It is worth mentioning that the highest variation in thickness from hanging-wall to footwall is recorded in Unit A (Late Pliocene-Quaternary) for fault F3. Conversely, faults F5 to F10 record EI values below 1.0 in Unit B (**Figure 11**).

5. Discussion

The interpretations in this work stress that Crotone's offshore basins were affected by major tectonic pulses, resulting in contrasting fault deformation styles since the Messinian Salinity Crisis. Each tectonic pulse is best understood within the broader framework of convergence between Africa and Europe, which dominated the Late Cenozoic evolution of the central Mediterranean Sea (Chamot-Rooke et al., 2005; Faccenna et al., 2001; 2004; Minelli and Faccenna, 2010; Polonia et al., 2011; Chizzini et al., 2025). Hence, this work recognizes for the first time the effect of two main tectonic stages in the CAW - separated by an episode of contractional/transpressional tectonics – that responded to collision between the NE Calabrian Arc and Apulian foreland. The seismic-stratigraphic marker separating these two main tectonic regimes is the MPCU - Mid-Pliocene Unconformity (Zecchin et al., 2012; 2015; 2020).

5.1 *Structural and depositional expressions of distinct tectonic regimes*

5.1.1 *Early Pliocene*

Structures and deformation styles affecting Lower Pliocene strata point out to a tectonic regime governed by interacting extensional and strike-slip faults. Evidence from seismic profiles and EI data suggest important extensional faulting just after the Miocene, whereby multiple half-grabens were filled by the Lower Pliocene Unit B (**Figures 5b, 6c and 11**). In fact, structural and stratigraphic features indicate, at this time, a tectonic regime that was primarily controlled by extension rather than pure strike-slip (**Figures 5b, 6c, and 7b**). This interpretation is also supported by the common strikes and relative parallelism of interpreted Lower Pliocene faults (**Figures 5d**), characters that contrast markedly with the conjugate or cross-cutting geometries typically observed in strike-slip fault systems (Peacock et al., 2017, Wu et al., 2018, Wu et al., 2020; Kumar et al., 2023; Ma et al., 2025). Such parallelism in faults is evident near fault F4, where the absence of linked fault segments commonly associated with strike-slip deformation further indicates extensional tectonics as being predominant in the Crotone Basin during the Lower Pliocene (**Figure 5d)**. Consequently, the small-scale folds observed in the immediate hanging-wall of faults F2, F11 and F12, expressed as a gentle warping of seismic reflections, are associated with local drag folding developed during normal-fault motion (**Figures 5b and 6c**). The presence of drag folds in these areas also suggests mechanical heterogeneity and strain partitioning across faults F2, F11 and F12 (Mohammedyasin et al. 2016). All in all, such geological features - linear and parallel fault arrays, the formation of tilt blocks and local drag folds - are consistent with predominant extensional tectonics. Furthermore, the N–S and NNW-SSE- and NE-SW strikes of main fault segments are not aligned with the expected NW-SE orientation of younger, regional-scale strike-slip structures (**Figure 4a**), indicating that Early Pliocene faults are unlikely to have developed as part of the major shear zones associated with the long-term tectonic evolution of the Calabrian Arc.

A single exception to extensional faulting is recorded along fault F1, where its reactivation promoted strike-slip movement along inherited structures that pre-date Early Pliocene extensional tectonics (**Figure 5a**). Such an observation pertaining to fault F1 concurs with the model proposed in **Mangano et al. (2023a**); faults along F1 reveal plan-view geometries that are sigmoidal and record systematic *en echelon* segmentation **(Figure 9).** In other words, the development of localized releasing stepovers and horsetail splays observed on attribute maps are diagnostic of a normal-oblique to strike-slip reactivation of F1 within an overall extensional regime (**Figure 9a**).

5.1.2 *Late Pliocene – Quaternary*

Upper Pliocene to Quaternary strata comprise multiple structures documenting strike-slip deformation. These structures mark a major shift between two fault deformation styles, i.e. from extensional to strike-slip tectonics. Based on the structural styles observed in seismic data, and the estimated EI plots, strike-slip motion was initiated in the Late Pliocene when faults became curved and some fault blocks (bounded by **F5 and F6**) formed pull-apart sub-basins, which are recognized as negative flower structures on selected seismic profiles (**Figures 5a and 9b**). Under such a transtensional regime, pull-apart sub-basins were developed in the study area along faults F7, F8, F9 and F10 **(Figure 6a,b)**. Adjacent to these, releasing stepovers can be observed and are characterized by a notable degree of fault parallelism and bending, reflecting localized zones of transtensional strain (**Figures 6a and 9a**). All these features are predominantly NW–striking **(Figure 9a)**. The new pull-apart sub-basins are typically narrow and elongated basins with a width/length ratio of 1:7, consistent with the morphology expected for transtensional basins (Mann et al., 2007) (**Figure 4b**). In such a context, the associated flower structures affecting Unit A (Late Pliocene-Quaternary) are linked to releasing beds and fault stepovers with *en echelon* fault segments in plan view (**Figures 5a and 9b**). Horsetail splays are additional structures suggesting strike-slip (see Mann et al., 2007), and occur as: a) fault segments curving away from master faults, and b) nearly linear splays that are subparallel to the principal zone of fault displacement (**Figure 9b**). The resulting divergent and variably curvilinear to subparallel fault splays reflect progressive block rotation and variations in displacement direction along master faults, indicating strike-slip deformation in a transtensional tectonic regime (Choi et al., 2016; Kim et al., 2003, 2004; McGrath & Davison, 1995; Mouslopoulou et al., 2007; Zampieri & Massironi, 2007).

Stratigraphically, Upper Pliocene-Quaternary strata in Unit A show variable thickness on both sides of faults F5 to F10 coming from NE to SW, indicating transtensional activity along this interval (**Figures 5a and 6a, b**). The extracted EI values further indicate important fault activity since the Late Pliocene; faults F5 to F10 record EI values that are consistently greater than 1, suggesting syn-tectonic growth (**Figure 11**). Evidence for syn-tectonic growth is also documented along fault F3, which appears to have acted as a conjugate segment between adjacent strike-slip structures. As shown in the variance time slice at T=1108 ms (**Figure 10b**), fault F3 exhibits a nearly linear geometry, lacks oblique splays, and is limited by sigmoidal fault traces that are typical of active strike-slip zones.

5.2 Geodynamic controls on the deformation styles

5.2.1 *Early Pliocene*

The formation of an extensional fault system in the Early Pliocene can be linked to gravitational collapse of an overthickened block of the overriding plate, itself inherited from Late Messinian contractional/transpressional tectonics. In line with the framework proposed by Dewey (1988), lithospheric extension is preferentially recorded along orogenic belts due to their anomalously thick continental crust, elevated topography, and internal structural heterogeneities. Extensional collapse is driven by body forces acting to restore isostatic equilibrium, particularly where sharp elevation gradients and rapid advective thinning of the lithospheric mantle combine to enhance uplift and crustal instability. The Crotone Basin, located along the internal margin of the CAW, offers an ideal setting for such a gravitational readjustment.

Crustal collapse in the Early Pliocene is therefore interpreted in this work as a direct consequence of the compressional phase that affected the CAW during the Late Messinian (Polonia et al., 2011; Chizzini et al. 2022; Butler, 2009; Basso et al., 2021; Volpi et al., 2017).

This time period was marked by basin inversion, with uplift and interruption of arc migration likely driven by collision between the Calabrian Arc and the Apulian foreland, a compressional regime that not only promoted thickening within the CAW but also propagated stress into the foreland, leading to salt mobilization, inversion of inherited extensional structures, and localized development of new deformation (Somma, 2006; Del Ben et al., 2010;Massari and Prosser, 2013; Volpi et al., 2017; Zecchin et al., 2020; Cicala et al., 2021; Chizzini et al., 2023). Such a compression led to rapid crustal thickening along the internal margin of the Calabrian Arc, setting the conditions for later extensional faulting.

Seismic profiles reveal the presence of broad, structurally controlled negative features just beneath faults F2, F11 and F12 where crustal thickening inferred from the Late Messinian compressional phase seems to have enhanced gravitational instability (**Figures 5b and 6c**). These subsiding domains, interpreted as inherited zones of lower crustal or lithospheric weakness, are interpreted as the preferential loci for vertical loading, ultimately promoting localized extension in response to crustal thickening. In such a setting, the formation of extensional structures in the Early Pliocene reflects the mechanical response of the orogenic crust to Late Messinian shortening, and gravitational spreading acted as the main driver of fault nucleation and upper crustal deformation. Renewed tectonic movements along inherited strike-slip structures thus relate to discrete pulses of stretching in the Crotone Basin that responded to the forward migration of the Calabrian Arc. They were also coeval with the initial oceanization of the Vavilov sub-basin in the Tyrrhenian back-arc region (Nicolosi et al., 2006; Guillaume et al., 2010; Zecchin et al., 2013; Zecchin et al., 2020).

5.2.2 *Late Pliocene – Quaternary*

The gradual imposition of a strike-slip tectonic regime after the Early Pliocene is documented in the study area by the formation of horsetail splays and negative flower structures that are subparallel to the strike of main faults (**Figure 9**)**.** They are also accompanied by the opening of local pull-apart sub-basins in the areas where transtensional strain was accommodated (Mann et al., 2007). The linear to gently curving fault splays aligned with the shear direction of master faults (e.g. faults F1, F5 and F6) are characteristic of Riedel Shears (see Mann et al. 2007; Cubas and Klinger, 2020 and reference therein), splaying out of strike-slip faults whenever shear is parallel to the fault plane but orthogonal to the curving splays (**Figure 9b**). These structures are typically associated with asymmetric stress fields. Conversely, fault splays oriented at high angles to a master fault are formed wherever shear is parallel both to the fault plane and to the splay itself, and reflect a more symmetric stress distribution around master faults (Atkinson, 1989; Choi et al., 2016; Dooley & Schreurs, 2012; Kim et al., 2003, 2004; McGrath & Davison, 1995) (**Figure 9**).

The spatial distribution of horsetail splays provides valuable insights into the direction of fault propagation. In particular, the occurrence of these splays on the footwall blocks suggests that master faults (e.g. faults F1, F5) propagated downward (**Figure 5a**). This interpretation aligns with previous studies demonstrating that horsetail splays forming in hanging-wall blocks typically reflect the upward propagation of fault tips, whereas their development on footwall blocks indicates a downward propagation (Friedman & Logan, 1970; McGrath & Davison, 1995; Del Ben et al., 2010). Hence, the geometric and spatial characters of horsetail splays not only reflect localized stress distribution at the fault tip, but also serve as kinematic markers of both the propagation direction and the oblique-slip nature of strike-slip systems.

Transtensional tectonics has dominated the study area since the Late Pliocene in the context of lateral fragmentation of the CAW's overriding slab. This resulted in varied fault displacements and the rotation of crustal blocks that are internal to the Calabrian Arc (Scheepers et al. 1993; Duermeijer et al. 1998; Van Dijk and Scheepers 1995). Normal-oblique strike-slip movements were accommodated by the Sibari and Catanzaro strike-slip faults, leading northern Calabria to change its movement from E to ESE (Del Ben et al., 2008) (**Figure 1a**). This process was controlled by the presence of two distinct foreland domains in terms of subduction resistance (i.e. continental Apulian and the oceanic Ionian), with the caveat that some authors interpret the Ionian plate as a hyper-extended continental crust (Platt and Vissers, 1989; Calvert et al., 2000).

Despite these alternative views, we favor an oceanic model in this work because recent wide-angle seismic, refraction, and potential-field data provide robust, internally consistent evidence for a thin (6–7 km), high-velocity crust and a shallow Moho beneath the Ionian Abyssal Plain - characteristics that are diagnostic of Mesozoic oceanic lithosphere. In particular, the velocity structure and Moho geometry documented by Dannowski et al. (2019) and the margin architecture and crustal affinities synthesized by Tugend et al. (2019) demonstrate that the Ionian Basin represents a preserved remnant of the Neo-Tethyan ocean domain. These findings align with earlier geophysical and geological studies supporting an oceanic crustal nature for the Ionian Basin (Finetti and Del Ben, 1986; Lanzafame and Bousquet, 1997; Gvirtzman and Nur, 1999; Argnani, 2000; Doglioni et al., 2001; Rosenbaum and Lister, 2004; Finetti, 2005). Despite the above crustal deformation processes, a relationship between transtensional tectonics along the Rossano-San Nicola Fault Zone and the left-lateral activation of the Sibari and Catanzaro strike-slip faults cannot be ruled out. Strike-slip movement along the Rossano-San Nicola Fault Zone can be referred as the development of conjugate structures in an *en echelon* arrangement with respect to the regional shear zone, which is WNW–ESE striking **(Figure 1a)**. Strike-slip movements after the Lower Pliocene were also concomitant with the fast spreading of the Marsili sub-basin in the CAW's backarc region, at a rate of *c.* 19 mm/year (Nicolosi et al., 2006). This phase of fast ocean spreading occurred together with inception of the southern sector of the Messina Strait (Del Ben et al., 2008). Therefore, the strike-slip tectonics documented in this work reflects the rheological asymmetry of the central Mediterranean foreland. Ultimately, the contrasting mechanical behaviors of the more rigid Apulian continental lithosphere relative to the denser (but more deformable) Ionian ocean domain, provide the fundamental control on the segmentation of the overriding plate and its Calabrian Arc.

6. Conclusions

This paper investigated the various deformation styles associated with episodic tectonic pulses affecting the offshore sector of the Crotone Basin after the Miocene. This was achieved via the interpretation and mapping of tectonic faults by using high-quality 3-D seismic reflection data. These data were tied to stratigraphic information gathered from nine (9) exploration boreholes, and were complemented by the measurement of Expansion Indices (EI) to quantify fault activity. The main conclusions from this work are summarized as follows:

a) Distributed extensional faulting started in the Early Pliocene in response to the gravitational collapse of an overthickened orogenic crust. This is better documented by the presence of N-striking normal faults and associated half-grabens, tilt blocks and local drag folds. Such normal faults are linear in plan view.

b) The presence of structurally controlled negative flower structures beneath some of the interpreted faults suggests a mechanical response to crustal instability inherited from Late Messinian shortening. Such an extensional tectonic style marks a post-collisional response to crustal overthickening produced by the convergence between the Calabrian Arc and the Apulian foreland.

c) Following the Late Messinian contractional/transpressional phase, crustal thickening and elevated topography drove vertical loading and orogenic extension along pre-existing structural weaknesses. This event was also concomitant with Ionian slab rollback, fast forward arc migration, and the onset of ocean spreading within the Vavilov sub-basin in the backarc area of the Calabrian Arc.

d) A transtensional regime took over the study area in the Late Pliocene due to the fragmentation of the overriding plate in response to the contrasting rheological behavior of adjacent foreland domains — the Apulian continental block and the Ionian oceanic lithosphere. This is demonstrated by the development of pull-apart zones and negative flower structures along NW– and NNW–striking fault zones.

e) Structural-kinematic indicators, including sigmoidal fault traces, releasing bends, horsetail splays, and *en echelon* fault arrangements, suggest a dominant normal oblique-slip mechanism consistent with the transition from extensional collapse to transtensional tectonics.

f) Notably, the Rossano-San Nicola Fault Zone may have acted as a conjugate structure of a regional WNW–ESE fault zones, forming part of a broader pattern of oblique deformation internal to the Calabrian Arc. This deformation style reflects the accommodation of differential displacement rates imposed by the contrasting rheological properties of the adjacent Apulian and Ionian forelands; a pattern consistent with a tectonic framework governed by lithospheric heterogeneity and diachronous foreland-arc interactions.

In summary, the evolution of the Crotone Basin reflects the interplay between regional convergence, slab rollback, and inherited structural fabrics. The transition from pure extension to oblique strike-slip faulting is closely linked to the differential subduction of heterogeneous foreland domains, and the dynamic evolution of the central Mediterranean backarc system as a whole.

Acknowledgments

Geophysical and geological data were generously supplied by ENI Natural Resources. We also thank Schlumberger for granting academic licenses for Petrel® software to the University of Calabria. We sincerely thank the Editor in Chief Federico Rossetti, the anonymous associate editor, reviewer D. Sakellariou, and two other anonymous reviewers, for their valuable and constructive comments, which improved the quality of the first submitted draft.

Open Research

Data availability. All data underlying the findings of this study are fully included in the main text and supplementary materials of this manuscript. Due to a confidentiality agreement with our industrial partner ENI NR, the raw data cannot be stored in a public repository.

Software availability. Structural modeling and visualization were performed using Petrel® software by Schlumberger. The software is proprietary and was used under an academic license granted to the University of Calabria. Petrel® is not publicly available for download. No custom scripts were developed for this study.

Conflict of interest statement

The authors have no conflicts of interest to disclose.

References

Argnani, A.(2000). The Southern Tyrrhenian subduction system: Recent evolution and neotectonic implication. *Annali di Geofisica*,43, 585–607

Atkinson, B. K.(Ed.). (1989).Fracture Mechanics of Rock. London: Academic Press

Basso, J., Artoni, A., Torelli, L., Polonia, A., Carlini, M., Gasperini, L. & Mussoni, P. (2021). Oblique plate collision and orogenic translation of the Southern Apennines revealed by post -Messinian interregional unconformities in the Bradano Basin (Ionian Sea - Central Mediterranean). *Marine and Petroleum Geology.* 128, 104999. https://doi.org/10.1016/j.marpetgeo.2021.104999

Barone, A., A. Fabbri, S. Rossi, & R. Sartori (1982). Geological structure and evolution of the marineareas adjacent to the Calabrian Arc, *Earth Evol.Sci*., 3, 207–221

Belayouni, H., Guerrera, F., Martin-Martin, M., Le Breton, E., & Tramontana, M. (2023).The Numidian formation and its lateral successions (Central-Western Mediterranean): A review. *International Geology Review*, 65(22), 3570-3602

Bird, P. (1979). Continental delamination and the Colorado Plateau. J*ournal of Geophysical Research: Solid Earth*, 84(B13), 7561-7571

Bonardi, G., Cavazza, W., Perrone, V., & Rossi, S. (2001). Calabria-Peloritani terrane and northern Ionian Sea. In: *Vai, G. B., & Martini, I. P. (Eds.), Anatomy of an Orogen: The Apennines and Adjacent Mediterranean Basins* (pp. 287–306). Kluwer Academic Publishers, Dordrecht, Netherlands

Borrelli, M., Perri, E., Critelli, S., Gindre-Chanu, L. 2021. The onset of the Messinian Salinity Crisis in the central Mediterranean recorded by pre-salt carbonate/evaporite deposition. *Sedimentology* 68, 1159–1197, doi: 10.1111/sed.12824.

Borrelli, M., Perri, E., Avagliano, D., Coraggio, F., Critelli, S., 2022. Paleogeographic and sedimentary evolution of North Calabrian basins during the Messinian Salinity Crisis (South Italy). *Marine and Petroleum Geology*, v. 141, Article number 105726, doi: 10.1016/j.marpetgeo.2022.105726.

Brown, A. R. (2004). Interpretation of three-dimensional seismic data (6th ed.). *AAPG Memoir 42, SEG Investigations in Geophysics*. Tulsa: American Association of Petroleum Geologists

Brown, A. (2004). Interpretation of Three-Dimensional Seismic Data, Sixth. ed. American Association of Petroleum Geologists (AAPG), Tulsa

Brune, S., Kolawole, F., Olive, J. A., Stamps, D. S., Buck, W. R., Buiter, S. J., .Furman, T. & Shillington, D. J. (2023). Geodynamics of continental rift initiation and evolution. *Nature Reviews Earth & Environment*, 4(4), 235-253

Brune, S., Williams, S. E., Butterworth, N. P., & Müller, R. D. (2023). Rift dynamics and architecture from 3D seismic: Examples from the Atlantic margins. *Tectonics*, 42(3), e2023TC007123

Butler, R.W.H. (2009). Relationships between the Apennine thrust belt, foredeep and foreland revealed by marine seismic data, offshore Calabria. *Boll. della Soc. Geol. Ital.* 128, 269–278. https://doi.org/10.3301/IJG.2009.128.2.269

Calvert, A., E. Sandvol, D. Seber, M. Barazangi, S. Roecker, T. Mourabit, F. Vidal, G. Alguacil, and N. Jabour (2000), Geodynamic evolution of the lithosphere and upper mantle beneath the Alboran region of the western Mediterranean: Constraints from travel time tomography, J. Geophys. Res., 105, 10,871 – 10,898.

Camerlenghi, A., Del Ben, A., Hübscher, C., Forlin, E., Geletti, R., Brancatelli, G., Micallef, A., Saule, M. & Facchin, L. (2020). Seismic markers of the Messinian salinity crisis in the deep Ionian Basin. *Basin Research* 32, 716–738. https://doi.org/10.1111/bre.12392

Cartwright, J. A., & Mansfield, C. S. (1998). Lateral displacement variation and lateral tip geometry of normal faults in the Canyonlands National Park, Utah. *Journal of Structural Geology*, 20(1), 3–19.https://doi.org/10.1016/S0191-8141(97)00079

Cavalcante, C., Fossen, H., Lagoeiro, L., & Taufner, R. (2024). The collapse of the Caledonian orogen in SW Norway: Insights from quartz textures. *Journal of Structural Geology*, 189, 105274

Cavazza, W., DeCelles, P.G., (1998). Upper Messinian siliciclastic rocks in southeastern Calabria (southern Italy): palaeotectonic and eustatic implications for the evolution of the central Mediterranean region. *Tectonophysics* 298, 223–241

Ceramicola, S., Cova, A., Forlin, E., Markezic, N., Mangano, G., Civile, D., Zecchin, M., Fanucci, F., Colizza, E., Corselli, C., Morelli, D., Savini, A., Caburlotto, A., Candoni, O., Coste, M., Cotterle, D., Critelli, S., Cuppari, A., Deponte, M., Dominici, R., Facchin, L., Gordini, E., Locatelli, M., Muto, F., Praeg, D., Romeo, R., & Tessarolo, C. (2024). Geohazard features of the Ionian Calabrian margin. *Journal of Maps*, 20(1), 2349785

Chamot-Rooke, N., Laigle, M., Gutscher, M.-A., & Klaeschen, D. (2005). The structural framework of the Calabrian Arc and Mediterranean Ridge. *Earth and Planetary Science Letters* 233, 1–18. https://doi.org/10.1016/j.epsl.2005.01.006

Chaumillon, E., & Mascle, J. (1997). From foreland to forearc domains: new multichannel seismic reflection survey of the Mediterranean Ridge accretionary complex (Eastern Mediterranean). *Marine Geology*, 138(3-4), 237-259

Chiarabba, C., De Gori, P. & Speranza, F. (2008). The southern Tyrrhenian subduction zone: deep geometry, magmatism and Plio-Pleistocene evolution. *Earth Planet Sci. Lett*. 268, 408–423

Chizzini, N., Artoni, A., Torelli, L., Polonia, A., Qadir, A., & Gasperini, L. (2025). Accretionary wedge collision in the Ionian Sea: Timing and movement of the Calabrian Arc and the Mediterranean Ridge in the central Mediterranean Sea. Gondwana Research 144, 212–238. https://doi.org/10.1016/j.gr.2025.04.011

Chizzini, N., Artoni, A., Torelli, L., Basso, J., Polonia, A. & Gasperini, L. (2022). Tectono-stratigraphic evolution of the offshore Apulian Swell, a continental sliver between two converging orogens (Northern Ionian Sea, Central Mediterranean). Tectonophysics 839. https://doi.org/10.1016/j.tecto.2022.229544

Chizzini, N., Artoni, A., Torelli, L., Maiorana, M., & Sulli, A. (2023). Evidence of new diapiric structures in the southern Adria Plate (Eastern Margin of Tethyan Ocean): Implications for Triassic paleogeography and evaporites remobilization during subduction/collision (Northern Ionian Sea, Central Mediterranean). Marine Geology 465. https://doi.org/10.1016/j.margeo.2023.107162

Choi, J. H., Edwards, P., Ko, K., & Kim, Y. S. (2016). Definition and classification of fault damage zones: A review and a new methodological approach. *Earth-Science Reviews*, 152, 70–87.https://doi.org/10.1016/j.earscirev.2015.11.006

Cicala, M., Festa, V., Sabato, L., Tropeano, M., & Doglioni, C. (2021). Interference between Apennines and Hellenides foreland basins around the Apulian swell (Italy and Greece). *Marine and Petroleum Geology* 133. https://doi.org/10.1016/j.marpetgeo.2021.105300

Civile, D., Mangano, G., Micallef, A., Lodolo, E., & Baradello, L. (2024). A Failed Rift in the Eastern Adventure Plateau (Sicilian Channel, Central Mediterranean). Journal of Marine Science and Engineering, 12(7), 1142

Civile, D., Zecchin, M., Tosi, L., Da Lio, C., Muto, F., Sandron, D., Affatato, A., Accettella, D., & Mangano, G. (2022). The Petilia-Sosti Shear Zone (Calabrian Arc, southern Italy): An onshore-offshore regional active structure. Marine and Petroleum Geology, 141, 105693

Critelli, S. & Criniti, S. (2021). Sandstone Petrology and Provenance in Fold Thrust Belt and Foreland Basin System, *in* Ali Ismail Al-Juboury , ed., Sedimentary Petrology - Implications in Petroleum Industry: Intech Open Access Publisher, Janeza Trdine 9, Rijeka, Croatia, p. 1-15, doi: 10.5772/intechopen.96985.

Critelli, S., & Martín-Martín, M. (2022). Provenance, paleogeographic and paleotectonic interpretations of Oligocene-Lower Miocene sandstones of the western-central Mediterranean region: A review. *Journal of Asian Earth Sciences*: X, 8, 100124

Critelli, S. & Martín-Martín, M. (2024). History of western Tethys Ocean and the birth of the circum-Mediterranean orogeny as reflected by source-to-sink relations. *International Geology Review*, v. 66 (2), p. 505-515**,** doi: 10.1080/00206814.2023.2280787.

Critelli, S. (1999). The interplay of lithospheric flexure and thrust accomodation in forming stratigraphic sequences in the southern Apennines foreland basin system, Italy. *Rendiconti Lincei* 10(4), 257-326

Critelli, S., Martín-Martín, M., Capobianco, W., & Perri, F. (2021). Sedimentary history and palaeogeographic of the Cenozoic clastic wedges of the Mal´ aguide Complex, Internal Betic cordillera Southern Spain. *Marine Petrol. Geol.* 124, 104775

Critelli, S., Perri, F., Arribas, J. & Herrero, M.J. (2018). Sandstone detrital modes and diagenetic evolution of Mesozoic continental redbeds from western-central circum-Mediterranean orogenic belts, *in* Ingersoll, R.V., Lawton, T.F., Graham, S., eds., Tectonics, Sedimentary Basins and Provenance: A Celebration of William R. Dickinson's Career: *Geological Society of America Special Paper 540*, p. 119-132 doi: 10.1130/2018.2540(06).

Cubas, N., & Klinger, Y. (2020). Experimental evidence for crustal control over seismic fault segmentation. https://doi.org/10.1130/G47115.1

Dalmayrac, B., & Molnar, P. (1981). Parallel thrust and normal faulting in Peru and constraints on the state of stress. *Earth and Planetary Science Letters*, 55(3), 473-481

Dannowski, A., Kopp, H., Klingelhoefer, F., Klaeschen, D., Gutscher, M. A., Krabbenhoeft, A. Dellong, D., Rovere, M., Graindorge, D., Papenberg, D., & Klaucke, I. (2019). Ionian Abyssal Plain: A window into the Tethys oceanic lithosphere. *Solid Earth*, *10*(2), 447-462.

Del Ben, A., Geletti, R., & Mocnik, A. (2010). Relation between recent tectonics and inherited Mesozoic structures of the central-southern Adria plate. *Boll. di Geofis. Teor. ed Appl.* 51, 99–115.

DeCelles, P.G., Cavazza, W., & (1995). Upper Messinian conglomerates in Calabria, southern Italy: response to orogenic wedge adjustment following Mediterranean sea-level changes. *Geology 23*, 775–778

Del Ben, A., Barnaba, C., & Taboga, A. (2008). Strike-slip systems as the main tectonic features in the Plio-Quaternary kinematics of the Calabrian Arc. *Mar. Geophys. Res*. 29, 1–12

Dewey, J. F. (1988). Extensional collapse of orogens. *Tectonics*, 7(6), 1123-1139

Dewey, J. F., Helman, M. L., Knott, S. D., Turco, E., & Hutton, D. H. W. (1989). Kinematics of the western Mediterranean. *Geological Society, London, Special Publications*, 45(1), 265-283

Doglioni, C. (1991). A proposal of kinematic modelling for W-dipping subductions-possible applications to the Tyrrhenian–Apennines system. Terra. Nova 3, 423–434

Doglioni, C., Innocenti, F., & Mariotti, G. (2001). Why Mt Etna?. *Terra Nova*, 13(1), 25-31

Dooley, T. P., & Schreurs, G. (2012). Analogue modelling of intraplate strike-slip tectonics: A review and new experimental results. *Tectonophysics*, 574, 1-71

Duermeijer, C. E., Van Vugt, N., Langereis, C. G., Meulenkamp, J. E., & Zachariasse, W. J. (1998). A major late Tortonian rotation phase in the Crotone basin using AMS as tectonic tilt correction and timing of the opening of the Tyrrhenian basin. *Tectonophysics*, 287(1-4), 233-249

Ebinger, C. J., Yemane, T., Woldegabriel, G., Aronson, J. L., & Walter, R. C. (1993). Late Eocene–Recent volcanism and faulting in the southern main Ethiopian rift. *Journal of the Geological Society*, 150(1), 99-108

Elliot, D. H., Larsen, D., Fanning, C. M., Fleming, T. H., & Vervoort, J. D. (2017). The Lower Jurassic Hanson Formation of the Transantarctic Mountains: implications for the Antarctic sector of the Gondwana plate margin. *Geological Magazine*, 154(4), 777-803

England, P. C., & Houseman, G. A. (1988). The mechanics of the Tibetan Plateau. *Philosophical Transactions of the Royal Society of London. Series A, Mathematical and Physical Sciences*, *326*(1589), 301-320.

Faccenna, C., Becker, T. W., Lucente, F. P., Jolivet, L., & Rossetti, F. (2001). History of subduction and back arc extension in the Central Mediterranean. *Geophysical Journal International*, 145(3), 809-820

Faccenna, C., Piromallo, C., Crespo-Blanc, A., Jolivet, L., & Rossetti, F. (2004). Lateral slab deformation and the origin of the western Mediterranean arcs. Tectonics, 23(1)

Feraud, G. (1990). 39Ar-40Ar analysis on basaltic lava series of Vavilov basin, Tyrrhenian sea (ocean drilling program, leg 107, holes 655B and 651A). In: In: Kastens, K.A., Mascle, J. (Eds.). *Proceedings of the Ocean Drilling Program, Scientific Results, vol. 107. Ocean Drilling Program, College Station, Texas*, pp. 93–97

Finetti IR (ed) (2005). CROP Project: deep seismic exploration of the Central Mediterranean and Italy. Atlases in Geoscience, vol 1. Elsevier

Finetti I, & Del Ben A (1986). Geophysical study of the Tyrrhenian opening. *Boll Geofis Teor Appl* 28(110):75–155

Finetti, I. (1982), Structure, stratigraphy and evolution of central Mediterranean. *Boll. Geofis. Teor. Appl.*,24, 247–312

Flecker, R., Krijgsman, W., Capella, W., de Castro Martíns, C., Dmitrieva, E., Mayser, J. P., Marzocchi, A., Modestou, S., Ochoa, D., Simon, D., Tulbure, M., van den Berg, B., van der Schee, M., de Lange, G., Ellam, R., Govers, R., Gutjahr, M., Hilgen, F., Kouwenhoven, T., Lofi, J., & Yousfi, M. Z. (2015). Evolution of the Late Miocene Mediterranean–Atlantic gateways and their impact on regional and global environmental change. *Marine Geology* 352, 25-58Gallais, F., Gutscher, M.-A., Klaeschen, D., & Graindorge, D. (2012). Two-stage growth of the Calabrian accretionary wedge in the Ionian Sea (Central Mediterranean): constraints from depth-migrated multichannel seismic data. *Marine Geology* 326–328, 28–45. https://doi.org/10.1016/j.margeo.2012.08.006

Gawthorpe, R. L., & Leeder, M. R. (2000). Tectono-sedimentary evolution of active extensional basins. *Basin Research*, 12(3-4), 195-218

Govers, R., Meijer, P., & Rijgsman, W. (2009). Regional isostatic response to messinian salinity crisis events. *Tectonophysics* 463, 109–129

Guerrera, F., & Martín-Martín, M. (2014). Geodynamic events reconstructed in the Betic, Maghrebian, and Apennine chains (central-western Tethys). *Bulletin de la Société géologique de France*, 185(5), 329-341

Guerrera, F., Martín-Algarra, A., & Martín-Martín, M. (2012). Tectono-sedimentary evolution of the 'Numidian Formation'and Lateral Facies (southern branch of the western Tethys): constraints for central-western Mediterranean geodynamics. *Terra Nova*, 24(1), 34-41

Guillaume, B., Funiciello, F., Faccenna, C., Martinod, J., & Olivetti, V. (2010). Spreading pulses of the Tyrrhenian sea during the narrowing of the calabrian slab. *Geology* 38, 819–822

Gvirtzman, Z., & Nur, A. (1999). The formation of Mount Etna as the consequence of slab rollback. *Nature*, 401(6755), 782-785

Gvirtzman, Z. & Nur, A. (2001). Residual topography, lithospheric structure and sunken slabs in the central Mediterranean. *Earth Planet Sci. Lett.* 187, 117–130

Heron, P. J., Pysklywec, R. N., & Stephenson, R. (2016). Lasting mantle scars lead to perennial plate tectonics. *Nature communications*, 7(1), 11834

Hilgen, F.J., Kuiper, K.F., Krijgman, W., Snel, E., & van der Laan, E. (2007). High-resolution integrated stratigraphy and astronomical tuning as prerequisites for deciphering the intricate history of the Messinian salinity crisis. *Stratigraphy* 4, 231–238

Hongxing, G., & Anderson, J. K. (2007). Fault throw profile and kinematics of Normal fault: conceptual models and geologic examples. *Geological Journal of China Universities*, 13(1), 75

Hosseinpour, M., Williams, S., Seton, M., Barnett-Moore, N., & Müller, R. D. (2016). Tectonic evolution of Western Tethys from Jurassic to present day: coupling geological and geophysical data with seismic tomography models. *International Geology Review*, 58(13), 1616-1645

Jackson, J., & McKenzie, D. (1983). The geometrical evolution of normal fault systems. *Journal of Structural Geology*, 5(5), 471-482

Kastens, K., Mascle, J., Auroux, C., Bonatti, E., Broglia, C., Channell, J., Curzi, P., Emeis, K-C., Glacon, G., Hasegawa, S., Hieke, W., Mascle, G., McCoy, F., McKenzie, J., Muller, J. M. C., Rehault, J-P., Robertson, A., Sartori, R., Sprovieri, R., & Torii, M. (1988). ODP Leg 107 in the Tyrrhenian Sea: Insights into passive margin and back-arc basin evolution. *Geological Society of America Bulletin,* 100(7), 1140-1156.

Kim, Y. S., Peacock, D. C. P., & Sanderson, D. J. (2003). Mesoscale strike-slip faults and damage zones at Marsalforn, Gozo Island, Malta. *Journal of Structural Geology*, 25(5), 793–812.https://doi.org/10.1016/S0191-8141(02)00200-Kim, Y. S., Peacock, D. C., & Sanderson, D. J. (2004). Fault damage zones. *Journal of Structural Geology*, 26(3), 503–517. https://doi.org/10.1016/ j.jsg.2003.08.002

Krijgsman, W., Capella, W., Simon, D., Hilgen, F. J., Kouwenhoven, T. J., Meijer, P. T., & Flecker, R. (2018). The Gibraltar corridor: Watergate of the Messinian salinity crisis. *Marine Geology*, 403, 238-246.

Krijgsman, W., Hilgen, F.J., Raffi, I., Sierro, F.J., & Wilson, D.S. (1999). Chronology, causes and progression of the Messinian salinity crisis. *Nature* 400, 652–655

Krijgsman, W., Rohling, E. J., Palcu, D. V., Raad, F., Amarathunga, U., Flecker, R.,Florindo, F., Roberts, A. P., Sierro, J. F., & Aloisi, G. (2024). Causes and consequences of the Messinian salinity crisis. *Nature Reviews Earth & Environment*, *5*(5), 335-350.

Kumar, P. C., Sain, K., & Omosanya, K. O. L. (2023). Geometry and Kinematics of strike-slip faults in the Dibrugarh field of the Upper Assam foreland basin, NE India. *Marine and Petroleum Geology*, 153, 106291

Labrousse, L., Prouteau, G., & Ganzhorn, A. C. (2011). Continental exhumation triggered by partial melting at ultrahigh pressure. *Geology*, 39(12), 1171-1174

Lanzafame, G., & Bousquet, J. C. (1997). The Maltese escarpment and its extension from Mt. Etna to Aeolian Islands (Sicily): importance and evolution of a lithosphere discontinuity. *Acta Vulcanologica*, 9, 113-120

Ma, B., He, Y., Chen, L., Wu, G., Dong, H., Wang, J., Yao, J.,, & Liu, X. (2025). Linkage, evolution and formation mechanism of the partially-thoroughgoing intra-cratonic conjugate strike-slip fault system in the northern Tarim Basin, NW China. *Journal of Asian Earth Sciences*, 106784.

Maesano, F.E., Tiberti, M.M., & Basili, R. (2017). The Calabrian Arc: Three-dimensional modelling of the subduction interface. *Scientific Reports* 7 (1), 1–15. https://doi.org/10.1038/s41598-017-09074-8

Malinverno, A., & Ryan, W. B. (1986). Extension in the Tyrrhenian Sea and shortening in the Apennines as result of arc migration driven by sinking of the lithosphere. *Tectonics*, 5(2), 227-245

Mangano, G., Alves, T. M., Zecchin, M., Civile, D., & Critelli, S. (2023). The Rossano–San Nicola Fault Zone evolution impacts the burial and maturation histories of the Crotone Basin, Calabrian Arc, Italy. *Petroleum Geoscience*, 29(2), petgeo2022-085

Mangano, G., Ceramicola, S., Alves, T. M., Zecchin, M., Civile, D., Del Ben, A., & Critelli, S. (2023a). A new large-scale gravitational complex discovered in the Gulf of Squillace (central Mediterranean): tectonic implications. *Scientific reports*, 13(1), 14695

Mangano, G., Ceramicola, S., Zecchin, M., Brancatelli, G., & Critelli, S. (2021, September). Geohazard-related geomorphic features in the Crotone-Spartivento Basin (Southern Italy): an expression of Calabrian Arc kinematics. In *Offshore Mediterranean Conference and Exhibition* (pp. OMC-2021). OMC

Mangano, G., Zecchin, M., & Civile, D. (2020). Large-scale gravity-driven phenomena in the Crotone Basin, southern Italy. *Marine and Petroleum Geology*, 117, 104386

Mangano, G., Zecchin, M., Civile, D., & Critelli, S. (2024). Tectonic evolution of the Crotone Basin (central Mediterranean): The important role of two strike-slip fault zones. *Marine and Petroleum Geology*, 163, 106769

Mangano, G., Zecchin, M., Civile, D., Ceramicola, S., Donato, A., Muto, F., Tripodi, V., & Critelli, S. (2022). Mid-miocene to recent tectonic evolution of the punta stilo swell (calabrian arc, southern Italy): an effect of calabrian arc migration. *Marine Geology*, 448, 106810

Mann, P., DeMets, C., & Wiggins-Grandison, M. (2007). Toward a better understanding of the Late Neogene strike-slip restraining bend in Jamaica: geodetic, geological, and seismic constraints.

Massari, F., & Prosser, G. (2013). Late Cenozoic tectono-stratigraphic sequences of the Crotone Basin: insights on the geodynamic history of the Calabrian arc and Tyrrhenian Sea. *Basin Research*, 25(1), 26-51

Mattei, M., Cifelli, F., & D'Agostino, N. (2007). The evolution of the Calabrian Arc: evidence from paleomagnetic and GPS observations. *Earth Planet Sci. Lett*. 263, 259–274

Mattei, M., Petrocelli, V., Lacava, D., & Schiattarella, M. (2004). Geodynamic implications of Pleistocene ultrarapid vertical-axis rotations in the Southern Apennines. Italy. *Geology* 32, 789–792

Mcculloh, R. P. (1988). Differential fault-related early Miocene sedimentation, Bayou Hebert area, southwestern Louisiana. *AAPG bulletin*, 72(4), 477-492

McGrath, A. G., & Davison, I. (1995). Damage zone geometry around fault tips. *Journal of Structural Geology*, 17(7), 1011–1024. https://doi.org/ 10.1016/0191-8141(94)00116-H

Meulenkamp, J. E., & Hilgen, F. J. (1986). Event stratigraphy, basin evolution and tectonics of the Hellenic and Calabro-Sicilian arcs. In *Developments in Geotectonics* (Vol. 21, pp. 327-350).

Minelli, L., & Faccenna, C. (2010). Evolution of the Calabrian accretionary wedge (central Mediterranean). *Tectonics*, 29(4)

Mitchum, R.M., Vail, P.R., & Thompson, S. (1977). Seismic stratigraphy and global changes of Sea level, Part 2: the depositional sequence as a basic unit for stratigraphic analysis. In: *Seismic Stratigraphy Applied to Hydrocarbon Exploration*, vol. 26. AAPG Memoir, pp. 53–62

Mohammedyasin, S. M., Lippard, S. J., Omosanya, K. O., Johansen, S. E., & Harishidayat, D. (2016). Deep-seated faults and hydrocarbon leakage in the Snøhvit Gas Field, Hammerfest Basin, southwestern Barents Sea. *Marine and Petroleum Geology*, 77, 160-178

Molnar, P., & Tapponnier, P. (1975). Cenozoic Tectonics of Asia: Effects of a Continental Collision: Features of recent continental tectonics in Asia can be interpreted as results of the India-Eurasia collision. *Science*, 189(4201), 419-426

Mouslopoulou, V., Nicol, A., Little, T. A., & Walsh, J. J. (2007). Displacement transfer between intersecting regional strike-slip and extensional fault systems. *Journal of Structural Geology*, 29(1), 100–116.https://doi.org/10.1016/j.jsg.2006.08.002

Mouslopoulou, V., Begg, J.G., Polonia, A., Nicol, A., Reston, T.J., Cesca, S., Giba, M., & Gasperini, L. (2025). Hellenic Subduction System and Upper-Plate Structures Revealed by Deep High-Resolution Seismic-Reflection Profiles and Seafloor Bathymetry. *Tectonics* 44. https://doi.org/10.1029/2025TC008943

Muto F., Spina V., Tripodi V., Critelli S., 2014, Tectonostratigraphic Neogene evolution of the allochthonous terrane in the Eastern Calabrian Foreland (Southern Italy). *Italian Journal of Geosciences*, v. 133, p. 455-473, doi: 10.3301/IJG.2014.23.

Nicolosi, I., Speranza, F., & Chiappini, M. (2006). Ultrafast oceanic spreading of the Marsili Basin, southern Tyrrhenian Sea: Evidence from magnetic anomaly analysis. *Geology*, 34(9), 717-720

Nicolosi, I., Speranza, F., Chiappini, M., 2006. Ultrafast oceanic spreading of the Marsili basin, southern Tyrrhenian Sea. Evidence from magnetic anomaly analysis. *Geology* 34, 717–720

Peacock, D. C. P., & Sanderson, D. J. (1991). Displacements, segment linkage and relay ramps in normal fault zones. *Journal of Structural Geology*, 13(6), 721-733

Peacock, D. C. P., Nixon, C. W., Rotevatn, A., Sanderson, D. J., & Zuluaga, L. F. (2017). Interacting faults. Journal of Structural Geology, 97, 1-22.

Peacock, D. C., & Sanderson, D. J. (1995). Strike-slip relay ramps. *Journal of Structural Geology*, 17(10), 1351-1360Platt, J. P., and R. L. M. Vissers (1989), Extensiona collapse of thickened continental lithosphere: A working hypothesis for the Alboran Sea and Gibraltar arc, Geology, 17, 540 – 543.

Pochat, S., Castelltort, S., Choblet, G., & Van Den Driessche, J. (2009). High-resolution record of tectonic and sedimentary processes in growth strata. *Marine and Petroleum Geology*, 26(8), 1350-1364

Pollock, J. (2025). The role of orogenic collapse on tectonic inheritance of passive continental margins. *Tectonics*, 44(1), e2023TC008207

Polonia, A., Camerlenghi, A., Davey, F., & Storti, F. (2002), Accretion, structural style and syncontrac-tional sedimentation in the eastern Mediterranean Sea. *Mar. Geol.,* 186, 127–144, doi:10.1016/S0025-3227(02)00176-7

Polonia, A., Torelli, L., Mussoni, P., Gasperini, L., Artoni, A., & Klaeschen, D. (2011). The Calabrian Arc subduction complex in the Ionian Sea: Regional architecture, active deformation, and seismic hazard. *Tectonics* 30. https://doi.org/10.1029/2010TC002821

Polonia, A., Torelli, L., Artoni, A., Carlini, M., Faccenna, C., Ferranti, L., Gasperini, L., Govers , R., Klaeschen, D., Monaco, C., Neri, G., Nijholt , N., Orecchio, B., & Wortel, R. (2016). The Ionian and Alfeo–Etna fault zones: New segments of an evolving plate boundary in the central Mediterranean Sea? *Tectonophysics*, 675, 69-90

Rosenbaum, G., & Lister, G. S. (2004). Neogene and Quaternary rollback evolution of the Tyrrhenian Sea, the Apennines, and the Sicilian Maghrebides. *Tectonics*, 23(1)

Rossetti, F., Goffé, B., Monié, P., Faccenna, C., & Vignaroli, G. (2004). Alpine orogenic P-T-t-deformation history of the Catena Costiera area and surrounding regions (Calabrian Arc, southern Italy): The nappe edifice of north Calabria revised with insights on the Tyrrhenian-Apennine system formation. *Tectonics*, 23(6)

Rossi, S., & Sartori, R. (1981). A seismic reflection study of the external Calabrian Arc in the northern Ionian Sea (eastern Mediterranean). *Marine Geophysical Researches*, 4(4), 403-426

Rossi, S., & Sartori, R. (1981). A seismic reflection study of the external Calabrian Arc in the northern Ionian Sea (eastern Mediterranean). *Marine Geophysical Researches*, 4(4), 403-426

Rouby, D., Guillocheau, F., Robin, C., Bouroullec, R., Raillard, S., Castelltort, S., Nalpas, T., & (2003). Rates of deformation of an extensional growth fault/raft system (offshore Congo, West African margin) from combined accommodation measurements and 3-D restoration. *Basin Res*. 15, 183e200

Royden, L. H. (1993). Evolution of retreating subduction boundaries formed during continental collision. *Tectonics*, 12(3), 629-638

Royden, L., & Faccenna, C. (2018). Subduction Orogeny and the Late Cenozoic Evolution of the Mediterranean Arcs. *Annual Review of Earth and Planetary Sciences* 46, 261–289. https://doi.org/10.1146/annurev-earth- 060115-012419

Roveri, M., Flecker, R., Krijgsman, W., Lofi, J., Lugli, S., Manzi, V., Sierro, F. J., Bertini, A., Camerlenghi, A., De Lange, G., Govers, R., Hilgen, F. J., Hübscher, C., Meijer, P. T., & Stoica, M. (2014). The Messinian Salinity Crisis: past and future of a great challenge for marine sciences. *Marine Geology*, 352, 25-58.

Sagnotti, L. (1992). Paleomagnetic evidence for a Pleistocene counterclockwise rotation of the Sant-Arcangelo Basin, southern Italy. *Geophys. Res. Lett*. 19, 135–138

Sartori, R. (1990). The main results of ODP Leg 107 in the frame of Neogene to Recent geology of peri-Tyrrhenian areas. In *Proceedings of the Ocean Drilling Program, Scientific Results* (Vol. 107, pp. 715-730)

Sawyer, D. S. (1985). Brittle failure in the upper mantle during extension of continental lithosphere. *Journal of Geophysical Research*, 90(B4), 3021–3025.https://doi.org/10.1029/JB090iB04p03021

Scheepers, P. J. J., Langereis, C. G., & Hilgen, F. J. (1993). Counter-clockwise rotations in the southern Apennines during the Pleistocene: paleomagnetic evidence from the Matera area. *Tectonophysics*, 225(4), 379-410

Scheepers, P.J.J., Langereis, C.G., Zijderveld, J.D.A., Hilgen, F.J., 1994. Paleomagnetic evidence for a Pleistocene clockwise rotation of the Calabro-Peloritan block (southern Italy). *Tectonophysics* 230, 19–48

Schettino, A., & Turco, E. (2011). Tectonic history of the western Tethys since the Late Triassic. *Bulletin*, 123(1-2), 89-105

Selverstone, J. (1988). Evidence for east-west crustal extension in the Eastern Alps: Implications for the unroofing history of the Tauern Window. *Tectonics,* 7(1), 87-105

Sioni, S. (1996), Mer Ionienne et Apulie depuis l'over-ture de l'Ocean Alpin, *Ph.D. thesis, Univ. de Bre-tagne Occidentale, Brest*

Somma, R. (2006). The south-western side of the Calabrian Arc (Peloritani Mountains): Geological, structural and AMS evidence for passive clockwise rotations. Journal of Geodynamics 41, 422–439. https://doi.org/10.1016/j.jog.2005.11.001

[Software] Schlumberger. (2024). Petrel® E&P Software Platform. Version 2024. Schlumberger Limited. https://www.software.slb.com/products/petrel

Spakman, W. (1986). Subduction beneath Eurasia in connection with the mesozoic tethys. *Geol. Mijnbouw* 65, 145–153

Speranza, F., Macrì, P., Rio, D., Fornaciari, E., & Consolaro, C. (2011). Paleomagnetic evidence for a post-1.2 Ma disruption of the Calabria terrane: consequences of slab breakoff on orogenic wedge tectonics. *Geol. Soc. Am. Bull*. 123, 925–933

Speranza, F., Mattei, M., Sagnotti, L., & Grasso, F., (2000). Rotational differences between the northern and southern Tyrrhenian domains: palaeomagnetic constraints from the Amantea basin (Calabria, Italy). *J. Geol. Soc. London* 157, 327–334

Strugale, M., & Cartwright, J. (2022). Tectono-stratigraphic evolution of the rift and post-rift systems in the Northern Campos Basin, offshore Brazil. *Basin Research*, 34(5), 1655-1687

Tapponnier, P., Zhiqin, X., Roger, F., Meyer, B., Arnaud, N., Wittlinger, G., & Jingsui, Y. (2001). Oblique stepwise rise and growth of the Tibet Plateau. *Science*, 294(5547), 1671-1677

Teyssier, C., Ferré, E. C., Whitney, D. L., Norlander, B., Vanderhaeghe, O., & Parkinson, D. (2005). Flow of partially molten crust and origin of detachments during collapse of the Cordilleran orogen. https://doi.org/10.1144/GSL.SP.2005.245.01.03

Thorsen, C. (1963). Age of growth faulting in Southeast Louisiana. Trans. *Gulf Coast Assoc. Geol. Soc*. 13, 103e110

Tugend, J., Chamot-Rooke, N., Arsenikos, S., Blanpied, C., & Frizon de Lamotte, D. (2019). Geology of the Ionian Basin and margins: A key to the East Mediterranean geodynamics. *Tectonics*, *38*(8), 2668-2702.

Van Dijk, J. P., & Scheepers, P. J. J. (1995). Neotectonic rotations in the Calabrian Arc; implications for a Pliocene-Recent geodynamic scenario for the Central Mediterranean. *Earth-Science Reviews*, 39(3-4), 207-246

Van Dijk, J. P., Bello, M., Toscano, C., Bersani, A., & Nardon, S. (2000). Tectonic model and three-dimensional fracture network analysis of Monte Alpi (southern Apennines). *Tectonophysics*, 324(4), 203-237

Van Dijk, J.P. (1991). Basin dynamics and sequence stratigraphy in the Calabrian Arc (central mediterranean): records and pathways of the Crotone Basin. *Geol. Mijnbouw* 70, 187–201

Van Dijk, J.P. (1994). Late Neogene kinematics of intra-arc oblique shear zones: the petiliaRizzuto fault zone (Calabrian Arc, central mediterranean). *Tectonics* 13, 1201–1230

Van Dijk, J.P., Bello, M., Brancaleoni, G.P., Cantarella, G., Costa, V., Frixa, A., Golfetto, F., Merlini, S., Riva, M., Torricelli, S., Toscano, C., & Zerilli, A. (2000). A regional structural model for the northern sector of the Calabrian Arc (southern Italy). *Tectonophysics* 324, 267–320

Van Dijk, J.P., & Okkes, F.W.M. (1991). Neogene tectonostratigraphy and kinematics of Calabrian basins; implications for the geodynamics of the Central Mediterranean. *Tectonophysics* 196, 23–60

van Hinsbergen, D.J.J., Torsvik, T.H., Schmid, S.M., Matenco, L.C., Maffione, M., Vissers, R.L.M., Gürer, D., & Spakman, W. (2020). Orogenic architecture of the Mediterranean region and kinematic reconstruction of its tectonic evolution since the Triassic. *Gondwana Research* 81, 79–229.https://doi.org/10.1016/j.gr.2019.07.009Wortel, M. J. R., & Spakman, W. (2000). Subduction and slab detachment in the Mediterranean-Carpathian region. *Science*, 290(5498), 1910-1917

Wu, G., Kim, Y. S., Su, Z., Yang, P., Ma, D., & Zheng, D. (2020). Segment interaction and linkage evolution in a conjugate strike-slip fault system from the Tarim Basin, NW China. Marine and Petroleum Geology, 112, 104054

Wu, G., Yuan, Y., Huang, S., Vandyk, T. M., Xiao, Y., Cai, Q., & Luo, B. (2018). The dihedral angle and intersection processes of a conjugate strike-slip fault system in the Tarim Basin, NW China. Acta Geologica Sinica-English Edition, 92(1), 74-88

Zampieri, D., & Massironi, M. (2007). Evolution of a poly-deformed relay zone between fault segments in the eastern Southern Alps, Italy. *Geological Society, London, Special Publications*, 290(1), 351–366.https://doi.org/10.1144/SP290.13

Zecchin M., Civile D., Caffau M., Muto F., Di Stefano A., Maniscalco R., & Critelli S., (2013a). The Messinian succession of the Crotone Basin (southern Italy) I: Stratigraphic architecture reconstructed by seismic and well data. *Marine and Petroleum Geology* 48, 455-473

Zecchin M., Caffau M., Di Stefano A., Maniscalco R., Lenaz D., Civile D., Muto F., & Critelli S., (2013b). The Messinian succession of the Crotone Basin (southern Italy) II: Facies architecture and stratal surfaces across the Miocene-Pliocene boundary. *Marine and Petroleum Geology* 48, 474-492

Zecchin, M., Accaino, F., Ceramicola, S., Civile, D., Critelli, S., Da Lio, C., Mangano, G., Prosser, G., Teatini, P., & Tosi, L. (2018). The Crotone Megalandslide, southern Italy: Architecture, timing and tectonic control. *Scientific reports*, 8(1), 7778

Zecchin, M., Caffau, M., Civile, D., Critelli, S., Di Stefano, A., Maniscalco, R., Muto, F., Sturiale, G., & Roda, C., (2012).The Plio-Pleistocene evolution of the Crotone Basin (southern Italy): interplay between sedimentation, tectonics and eustasy in the frame of Calabrian Arc migration. *Earth-Science Reviews* 115(4), 273-303

Zecchin, M., Civile, D., Caffau, M., Critelli, S., Muto, F., Mangano, G., & Ceramicola, S. (2020). Sedimentary evolution of the Neogene-Quaternary Crotone Basin (southern Italy) and relationships with large-scale tectonics: A sequence stratigraphic approach. *Marine and Petroleum Geology*, 117, 104381

Zecchin, M., Mellere, D., & Roda, C., (2006). Sequence stratigraphy and architectural variability in growth fault-bounded basin fills: a review of Plio-Pleistocene stratal units of the Crotone Basin, southern Italy.J. *Geol. Soc. London* 163, 471–486

Zecchin, M., Praeg, D., Ceramicola, S., & Muto, F., (2015). Onshore to offshore correlation of regional unconformities in the Plio-Pleistocene sedimentary successions of the Calabrian Arc (central Mediterranean). *Earth-Science Reviews* 142, 60-78

Figure captions

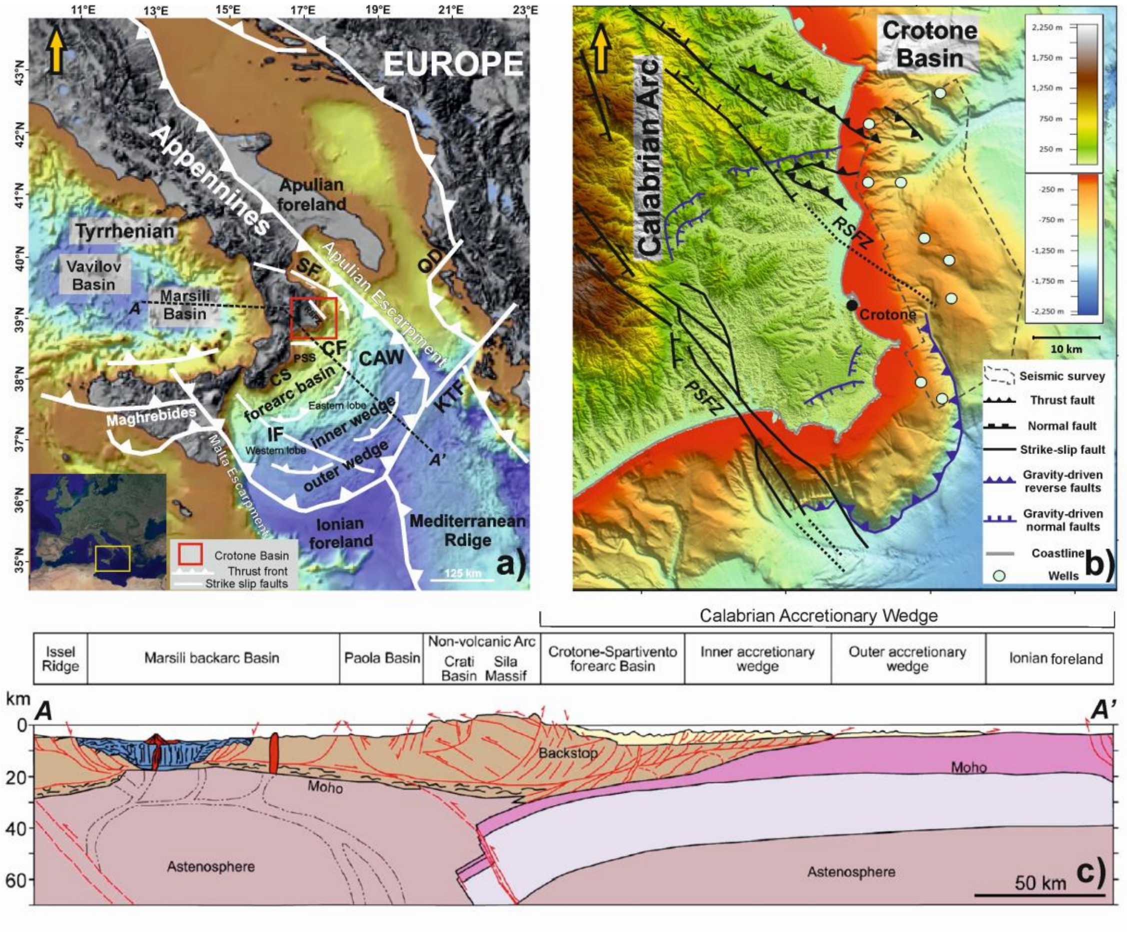

Figure 1. a) Present-day structural map of the Central Mediterranean region showing the Calabrian Accretionary Wedge and its backarc area. The inset highlights its location in the middle part of the Mediterranean Sea. CAW: Calabrian Accretionary Wedge; CS: Crotone-Spartivento; CF: Catanzaro Fault; IF: Ionian Fault System; KFT: Kefalonia Transfer Zone; OD: Othoni-Dhermi; RSFZ: Rossano-San Nicola Fault Zone; SF: Sibari Fault Source: CGMW and UNESCO (2012). b) Present-day structural map of the Crotone Basin, which is crosscut by the two fault zones: the Rossano-San Nicola Fault Zone (RSFZ) and the Petilia Sotisi Fault Zone (PSFZ). The location of the seismic volume used in this study is show in the figure. Onshore data are derived from: SRTM (Shuttle Radar Topography Mission) worldwide digital elevation data with 30 m (1 arc-second) resolution, released by NASA (SRTM PLUS Version 3.0) and made available by the U.S. Geological Survey (https://lpdaac.usgs.gov/search/), and Tin Italy DEM, a digital elevation model of the whole Italian territory available as a 10 m cell size grid (Tarquini et al., 2012, 2012; http://tinitaly.pi.ingv.it/Download_Area2.html). Bathymetric data are derived from the EMODnet Digital Terrain Model with a 1/16 * 1/16 arc minutes grid resolution (about 115-115 m) and extracted from https://emodnet.ec.europa.eu/en/bathymetry. The vector data (coastline) are derived from Copernicus, which is the European Union's earth observation program based on satellite and in situ observations (https://land.copernicus.eu/imagery-in-situ/eu-hydro/eu-hydro-river-network-database). c) NW-SE section across the CAW, showing main structural elements and its back-arc area (modified from Van Dijk et al., 2000).

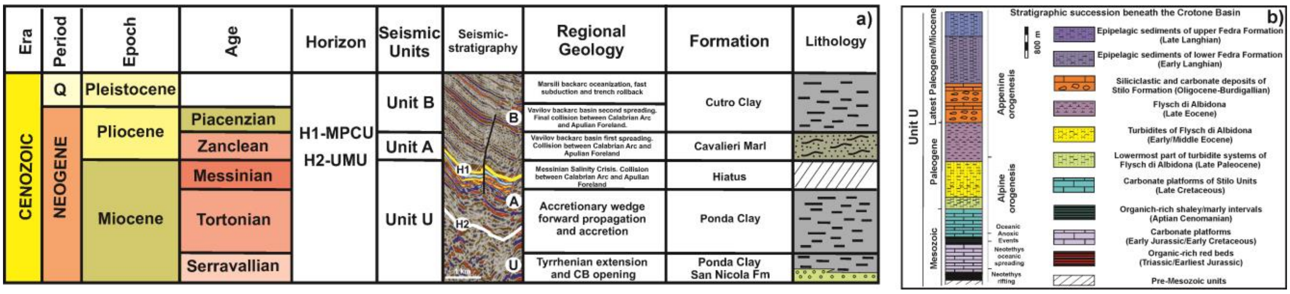

Figure 2. a) Lithological and seismic stratigraphic column with the ages, lithology, and regional tectonic events that marked the evolution of the Crotone Basin from the Middle Miocene (Serravallian) to the present day. Main seismic-stratigraphic horizons interpreted in this study are named horizons H1 to H2, which correspond to the MPCU and UMU. They bound Units A, B and U. Hence, the interval of interest to this study spans from the San Nicola Formation (Serravallian) to the Cutro Clay (Piacenzian-Quaternary). b) Triassic–upper Langhian strata, occurring beneath the Mid-Miocene–Quaternary Crotone Basin, composing most of the seismic-stratigraphic Unit U (modified from Mangano et al., 2023a).

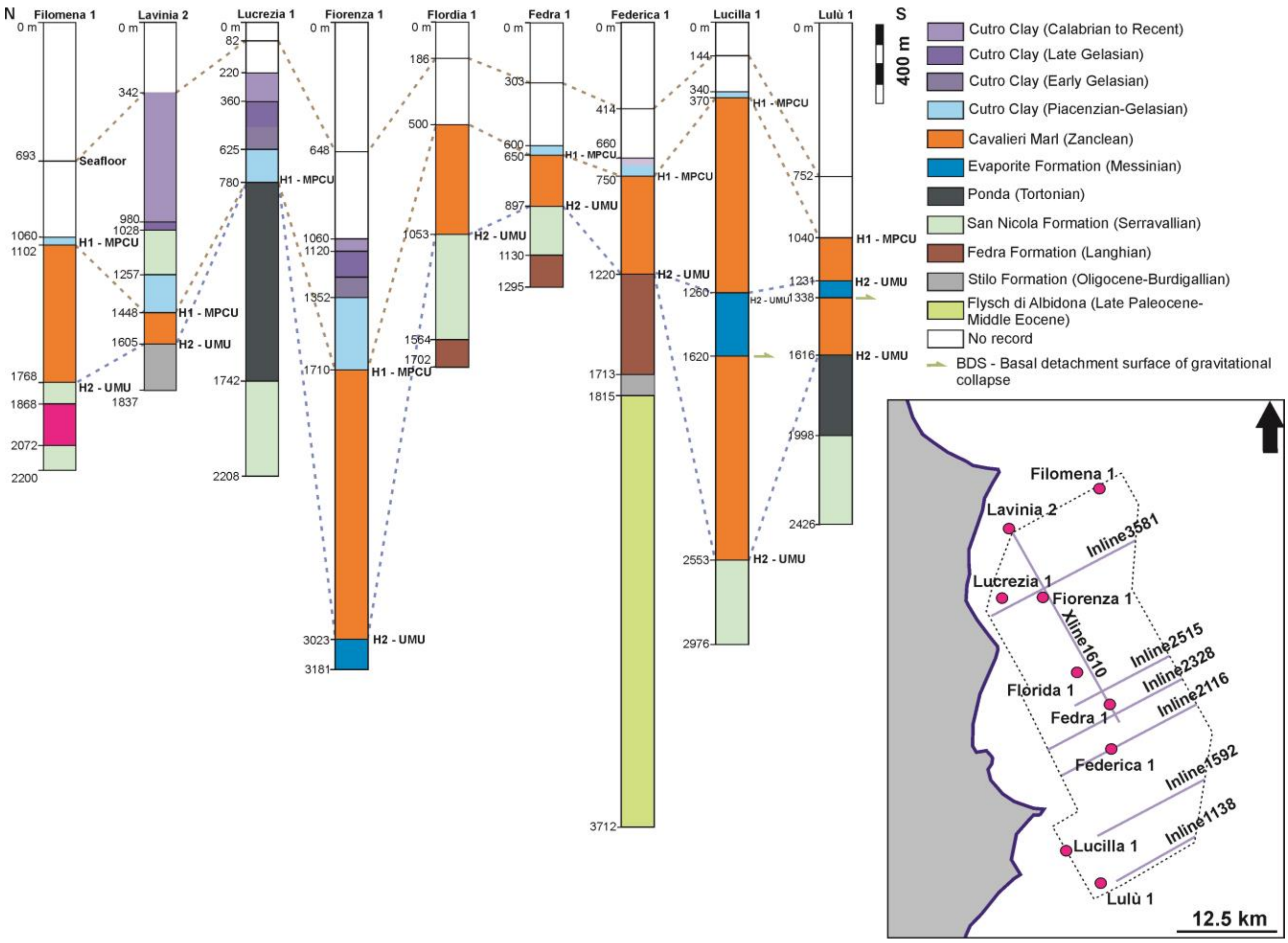

Figure 3. Panel correlating lithologies and ages of stratigraphic units in the study area. Inset highlights the wells and seismic sections interpreted in this paper.

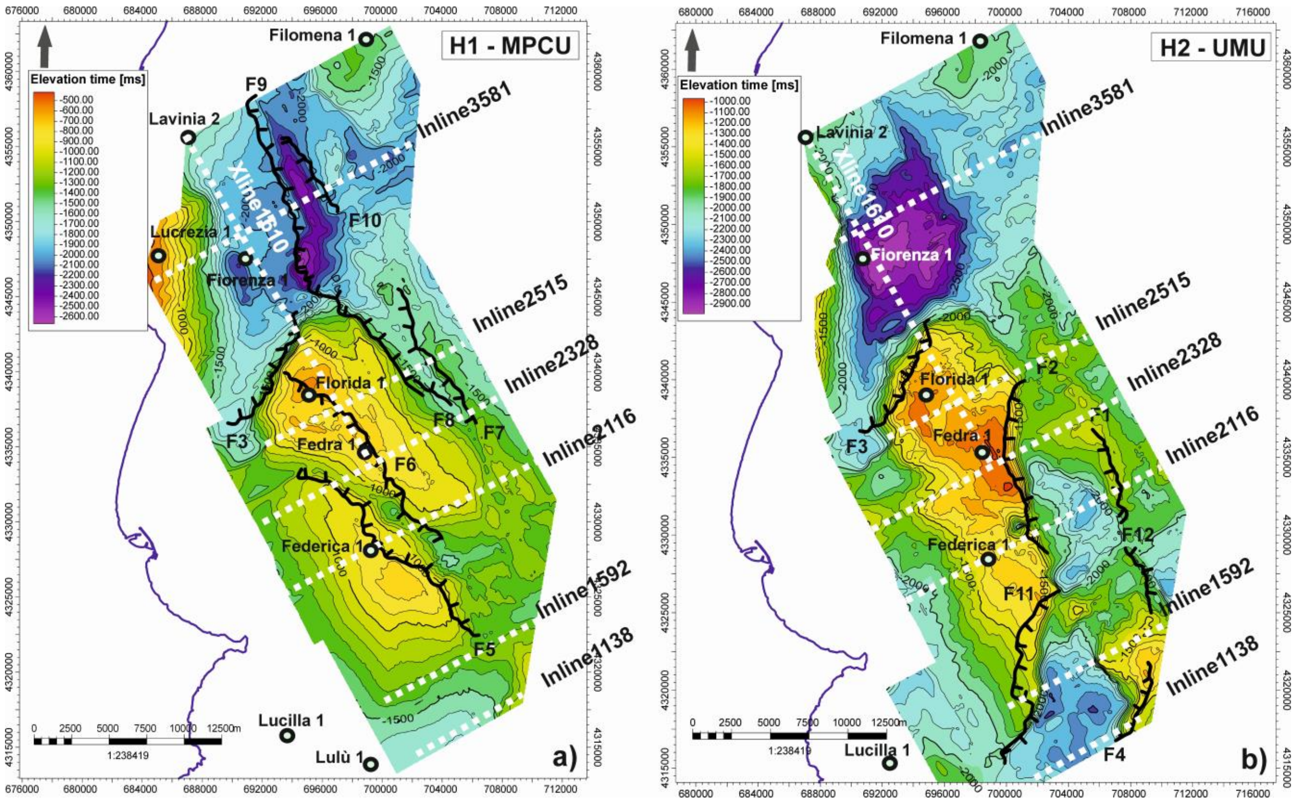

Figure 4. Two-way-time (TWT) structural maps of horizon H1 associated with MPCU, and horizon H2 corresponding to UMU. a) Horizon H1 reveals a narrow and elongated NW-SE oriented depocenter, bounded by transtensional faults, that reaches a depth of c. 2600 ms TWT. B) Horizon H2 significantly deepens to more than 2900 ms (TWT) and is offset by extensional/transtensional faults.

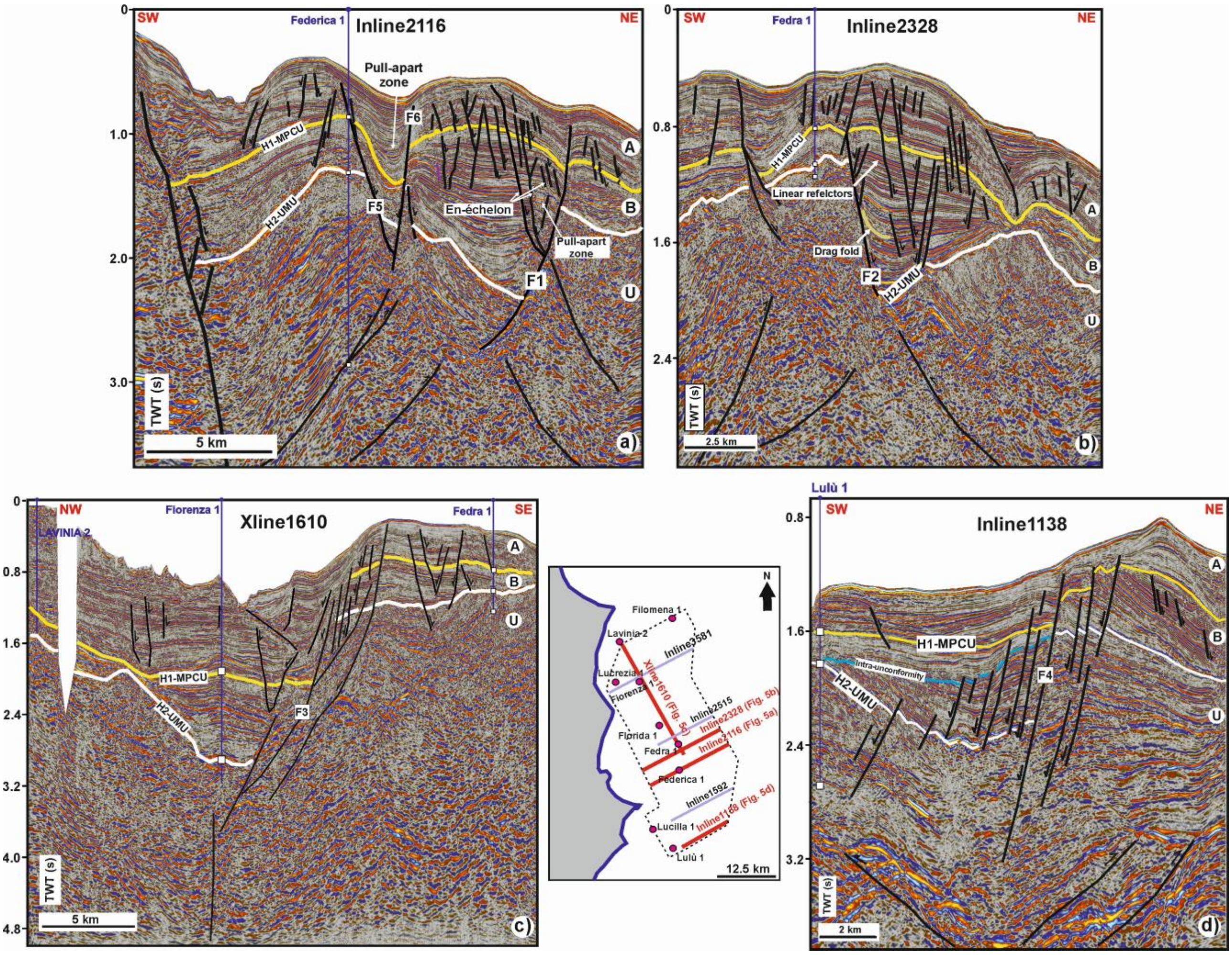

Figure 5. Interpreted seismic sections a) Inline 2116, b) Inline 2328, c) Xline 1610 and d) Inline 1138 highlighting the tectonic styles in the Crotone Basin. a) Faults F1, F5 and F6 crosscut Units A, B and U to reveal a divergent geometry towards their upper tips and a curved *en echelon* geometry in plan view. b) Inline 2328 shows linear reflectors with drag folds related to normal offsets along fault F2, whose upper tips lie beneath the MPCU. c) Fault F3 is a normal fault with marked splaying on its footwall block. It was likely reactivated as a conjugate fault during strike-slip motion. d) Fault F4 is part of a normal fault array with a clear structural parallelism. Faults are marked using solid black-colored lines. UMU: Upper Messinian Unconformity. MPCU: Mid-Pliocene unconformity. Unit A: Late Pliocene-Quaternary; Unit B: Early Pliocene; Unit U: pre-Pliocene. The uninterpreted seismic sections are provided as supplementary files.

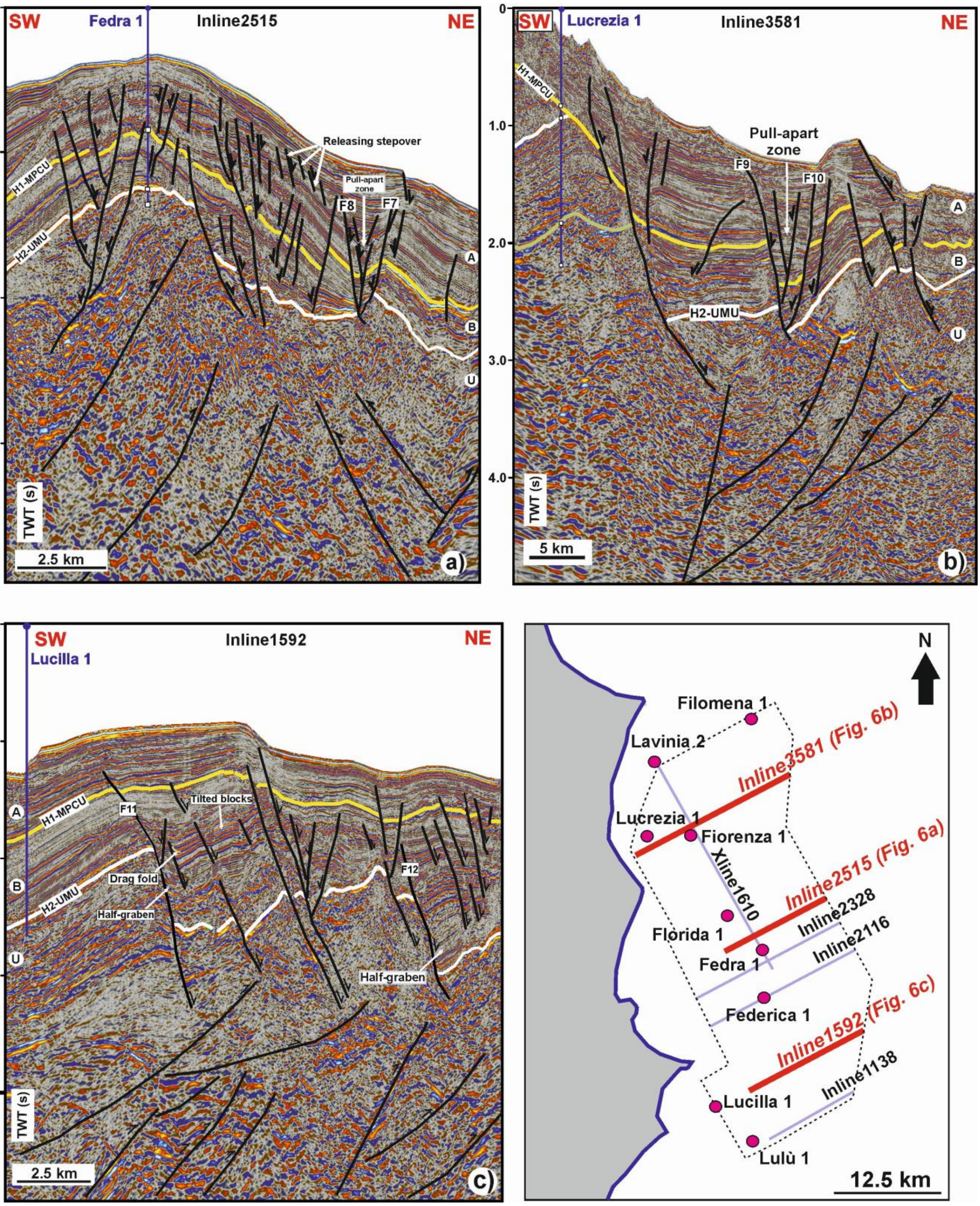

Figure 6. Geoseismic sections of a) Inline 2515, b) Inline 3581 and c) Inline 1592. a) Inline 2515 and b) Inline 3581 showing main structures along F7 to F10 and associated with pull-apart zones in this work. c) Inline 1592 highlighted the presence of faults F11 and F12 to be restricted to Unit B. Fault geometry includes half-graben and tilt blocks, and both structures are sub-parallel. Faults are marked using solid black-colored lines. UMU: Upper Messinian Unconformity. MPCU: Mid-Pliocene unconformity. Unit A: Late Pliocene-Quaternary; Unit B: Early Pliocene; Unit U: pre-Pliocene. The uninterpreted seismic sections are provided as supplementary files.

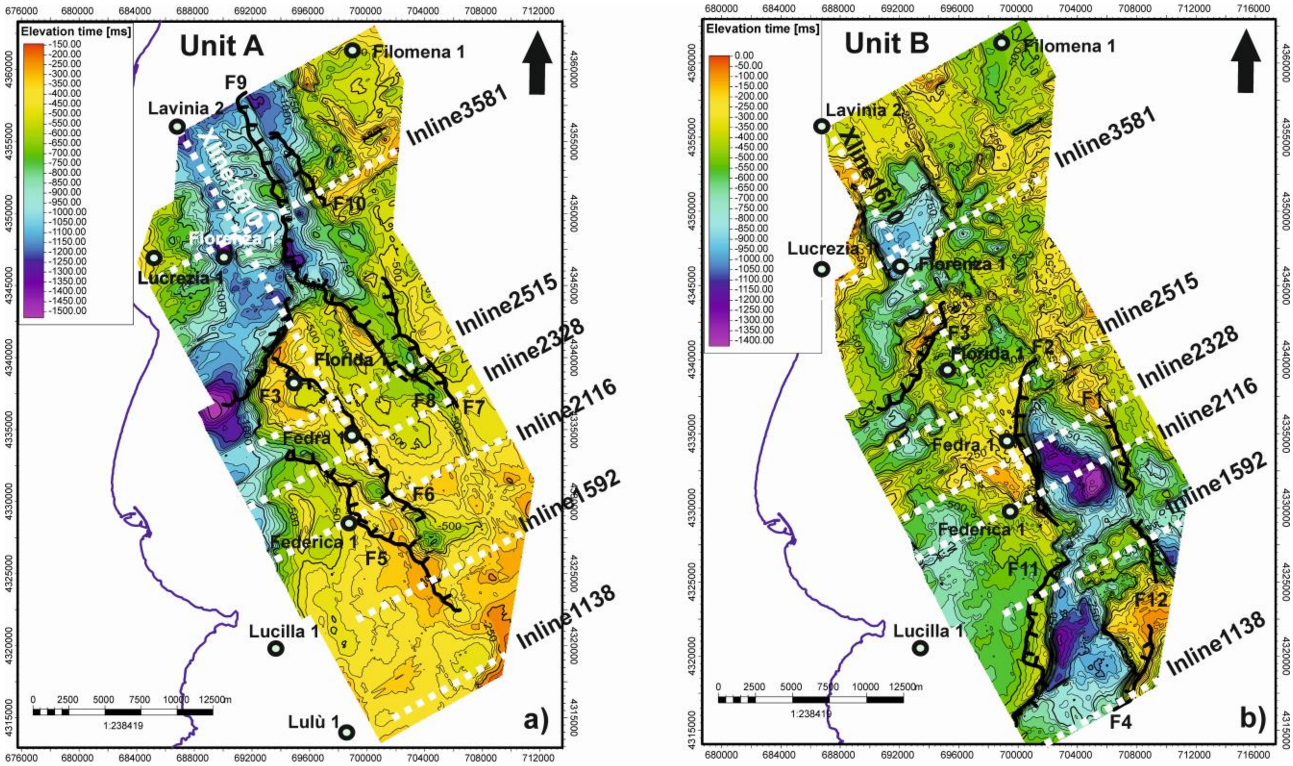

Figure 7. Isochron thickness of: a) Unit A (Late Pliocene-Quaternary), and b) Unit B (Early Pliocene). a) Unit A reveals the thickest strata in the northern sector of the study area, where it is affected by transtensional faults. b) In the central and southern sectors there are two regions bounded by extensional faults in which Unit B is thicker.

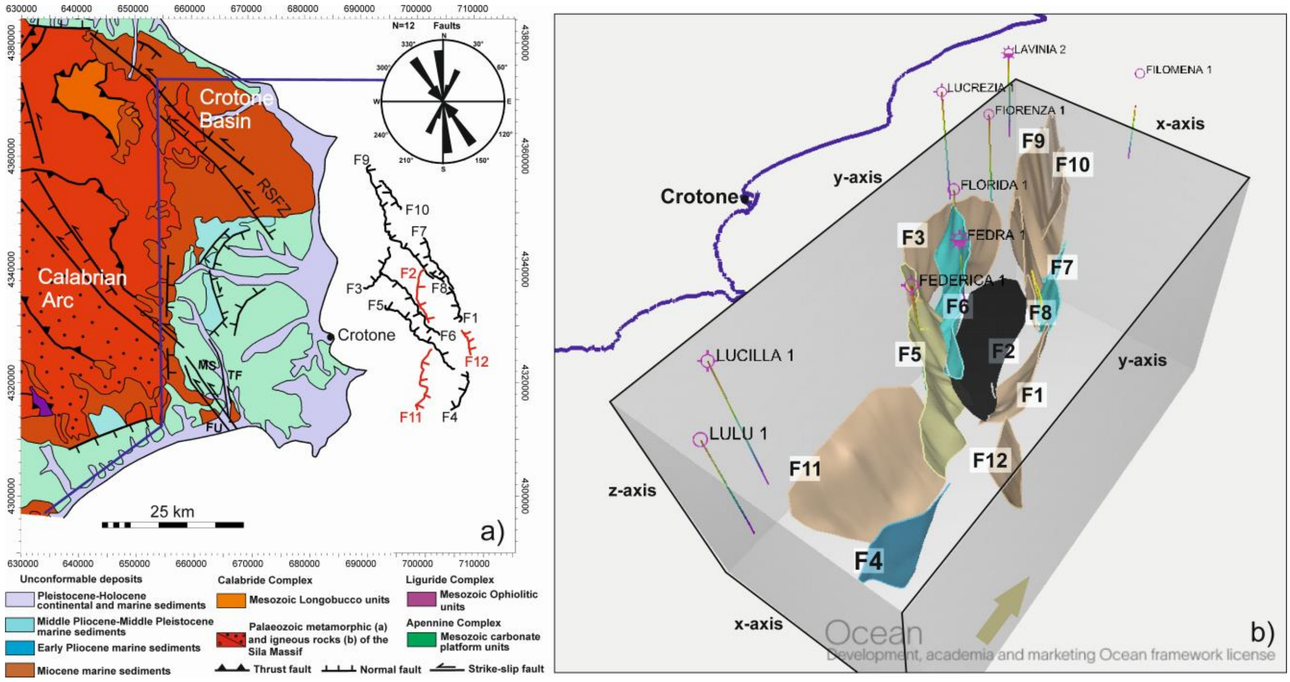

Figure 8. a) Structural map of the Calabrian Arc combined with the onshore geology of the Crotone Basin (modified after Van Dijk and Okkes, 1991). The figure highlights the location of the Rossano–San Nicola Fault Zone (RSFZ), plus the Marcedusa-Steccato (MS), the Tacina (TF) and Fosso Umbro (FU) faults that form the larger Petilia Sosti Fault Zone (PSFZ). The 12 faults (F1 to F12) mapped in this work are also shown in the figure. Faults marked as red-colored segments (F2, F11, F12) are quiescent at present, while those represented by black-colored segments (F1, F3 to F10) show signs of activity in seismic data. A rose diagram shows that the strike of the interpreted faults ranges from approximately N20 to N176. b) Three-dimensional view of the 12 faults interpreted in this work. Vertical exaggeration is 5x in the figure.

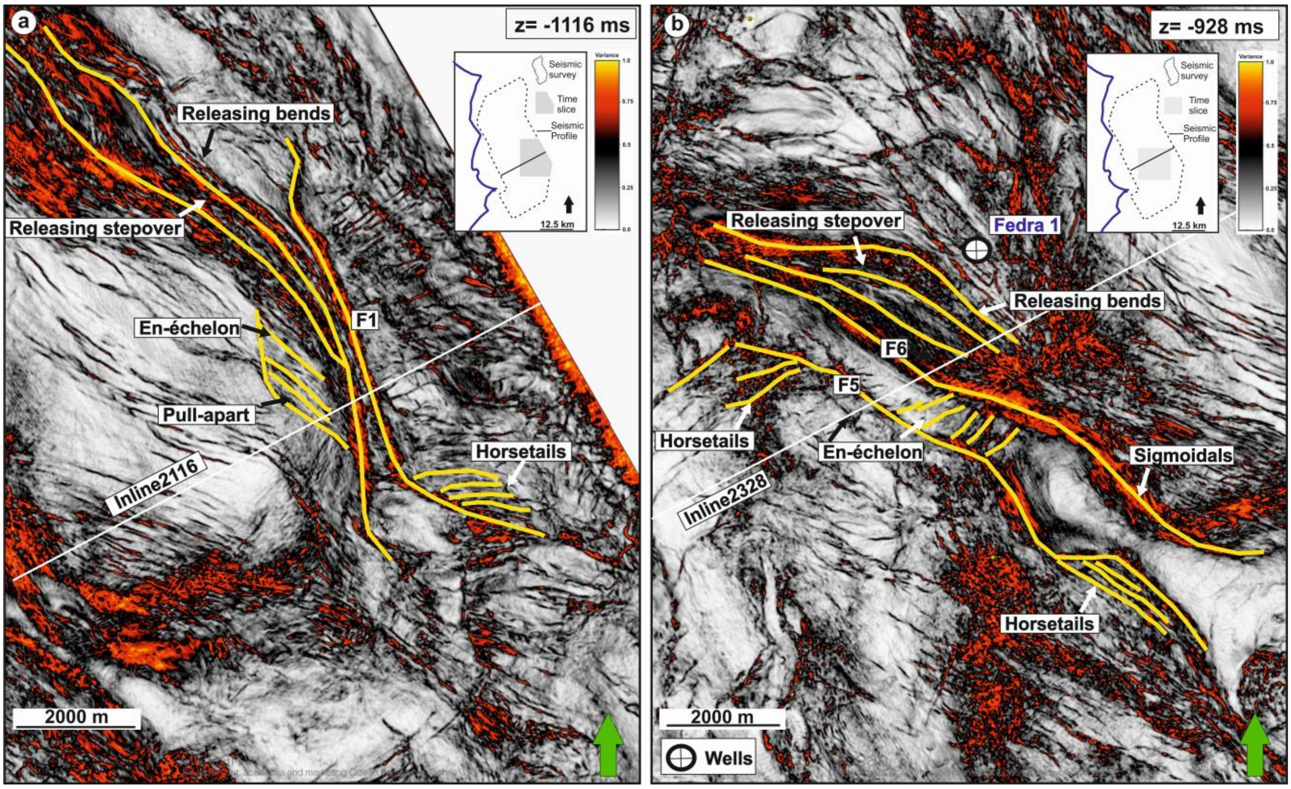

Figure 9. Variance time-slices extracted at a TWT depth of a) -1116 ms and b) -928 ms. Faults F1, F5 and F6 show several structural indicators such as sigmoidal geometries in faults as well as splay faults that are oblique and parallel to main fault segments.

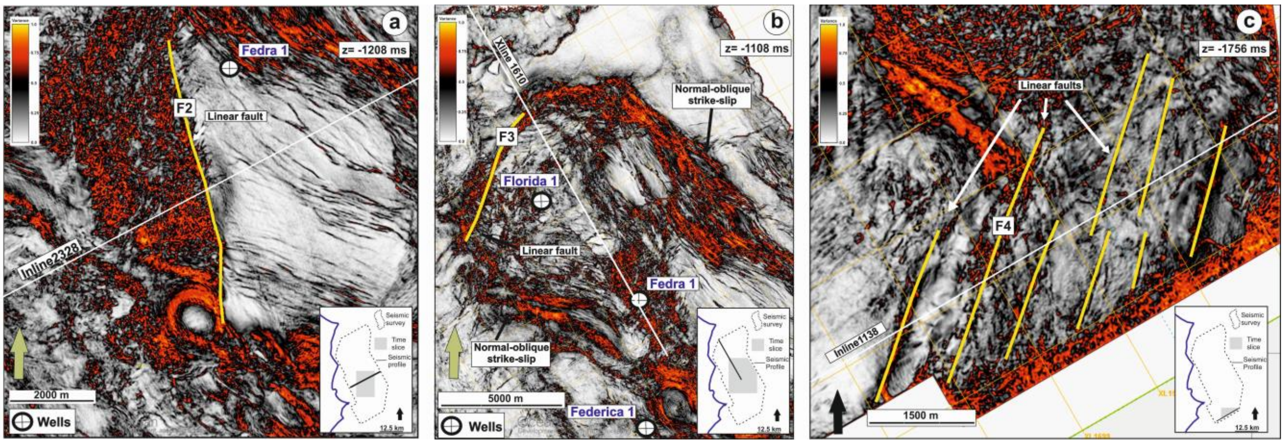

Figure 10. Variance time-slices extracted at a TWT depth of a) -1208 ms, b) -1108 ms and c) -1756 ms highlighting the geometry of faults F2, F3 and F4. They form discrete segments that strike N-S and NE-SW in Fig. 4a. The faults are linear in plan view, whereas F3 appears as a conjugate fault for the normal strike-slip faults in Fig. 10b. c) Fault F4 shown as part of a subparallel network of faults.

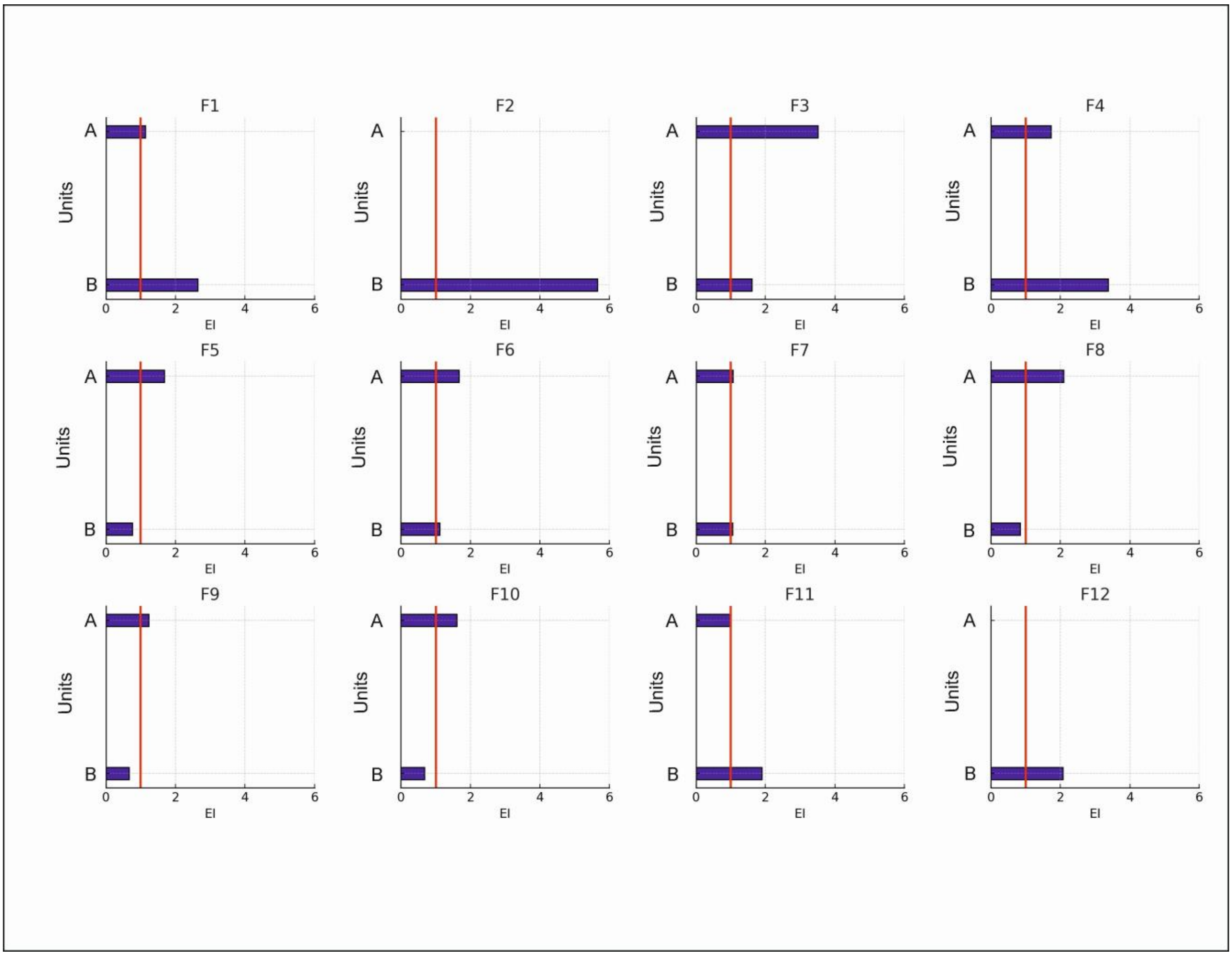

Figure 11. Expansion index (EI) for the faults interpreted in this work. Faults F1, F2, F4, F11, and F12 show EI values that exceed 1 along Unit B, whereas they show values close to or below 1 in Unit A. In contrast, faults F5 to F10 record EI values well above 1 in Unit A, changing to an EI close to 1 in Unit B. N.B: The red line marks the position of expansion index values (EI) equivalent to 1.